Non-invasive stimulation of the human striatum disrupts reinforcement learning of motor skills

Pierre Vassiliadis[1,2,3], Elena Beanato[1,2], Traian Popa[1,2], Fabienne Windel[1,2], Takuya Morishita[1,2], Esra Neufeld[4], Julie Duque[3], Gerard Derosiere[3,5], Maximilian J. Wessel[1,2,6] and Friedhelm C. Hummel[1,2,7 *]

[1]Defitech Chair of Clinical Neuroengineering, Neuro-X Institute (INX) and Brain Mind Institute (BMI), École Polytechnique Fédérale de Lausanne (EPFL), 1202 Geneva, Switzerland.

[2]Defitech Chair of Clinical Neuroengineering, INX and BMI, EPFL Valais, Clinique Romande de Réadaptation,1951 Sion, Switzerland.

[3]Institute of Neuroscience, Université Catholique de Louvain, 1200, Brussels, Belgium

[4]Foundation for Research on Information Technologies in Society, Zurich, Switzerland

[5]Lyon Neuroscience Research Center – Impact team - Inserm U1028 – CNRS UMR5292, Lyon 1 University, Bron, France

[6]Department of Neurology, University Hospital, Julius-Maximilians-University, Würzburg, Germany

[7]Clinical Neuroscience, University of Geneva Medical School, 1202 Geneva, Switzerland.

*** CORRESPONDENCE TO:**

Friedhelm C. Hummel

Neuro-X Institute (INX)

École Polytechnique Fédérale de Lausanne (EPFL)

Campus Biotech, Room H4.3.132.084

Chemin des Mines 9, 1202 Geneva, Switzerland

and

EPFL Valais,

Clinique Romande de Réadaptation

Av. Grand-Champsec 90,

CH-1951 Sion

Email: friedhelm.hummel@epfl.ch

Abstract

Reinforcement feedback can improve motor learning, but the underlying brain mechanisms remain underexplored. Especially, the causal contribution of specific patterns of oscillatory activity within the human striatum is unknown. To address this question, we exploited an innovative, non-invasive deep brain stimulation technique called transcranial Temporal Interference Stimulation (tTIS) during reinforcement motor learning with concurrent neuroimaging, in a randomised, sham-controlled, double-blind study. Striatal tTIS applied at 80Hz, but not at 20Hz, abolished the benefits of reinforcement on motor learning. This effect was related to a selective modulation of neural activity within the striatum. Moreover, 80Hz, but not 20Hz tTIS increased the neuromodulatory influence of the striatum on frontal areas involved in reinforcement motor learning. These results show for the first time that tTIS can non-invasively and selectively modulate a striatal mechanism involved in reinforcement learning, opening new horizons for the study of causal relationships between deep brain structures and human behaviour.

Keywords:

Motor learning, reward, reinforcement learning, non-invasive brain stimulation, deep brain stimulation, temporal interference stimulation, striatum, neuroimaging

1. Introduction

The ability to learn from past outcomes, often referred to as reinforcement learning, is fundamental for complex biological systems[1]. Reinforcement learning has been classically studied in the context of decision making, when agents have to decide between a discrete number of potential options[2]. Importantly, there is an increasing recognition that reinforcement learning processes are also at play in other contexts including during practice of a new motor skill[3–5]. For instance, the addition of reinforcement feedback during motor training can improve motor learning, presumably by boosting the retention of newly acquired motor memories[6,7]. Interestingly, reinforcement feedback also appears to be relevant for the rehabilitation of patients suffering from motor impairments[8–10]. Yet, despite these promising results, there is currently a limited understanding of the brain mechanisms that are critical to implement this behaviour.

A prominent hypothesis in the field is that the striatum, a structure that is particularly active both during reinforcement[11] and motor learning[12], may be causally involved in the beneficial effects of reinforcement on motor learning. As such, the striatum shares dense connexions with dopaminergic structures of the midbrain as well as with pre-frontal and motor cortical regions[13], and is therefore well positioned to mediate reinforcement motor learning[14–16]. This idea is supported by neuroimaging studies showing reward-related activation of the striatum during motor learning[17,18]. More specifically, within the striatum, oscillatory activity in specific frequency bands is suggested to be involved in aspects of reinforcement processing. Previous rodent studies have shown that striatal high gamma oscillations (~ 80 Hz) transiently increase following reward delivery[19–23], but not when reward is withheld[19]. Hence, dynamic changes of high gamma activity in the striatum[19,24,25] and in other parts of the basal ganglia[26,27] may encode the outcome of previous movements (i.e., success or failure) and support learning. Consistent with a role of such oscillatory activity in reinforcement learning, high gamma activity in the striatum shows coherence with frontal cortex oscillations and is up-regulated by dopaminergic agonists[19]. Hence, this body

of work suggests that reinforcement-related modulation of striatal oscillatory activity, especially in the gamma range, may be crucial for reinforcement learning of motor skills. Conversely, striatal beta oscillations (~20 Hz) have been largely associated with sensorimotor functions[28]. For instance, beta oscillations in the striatum are exacerbated in Parkinson's disease and associated to the severity of motor symptoms[29–31]. Consistently, excessive beta connectivity is reduced by anti-parkinsonian treatment in proportion to the related motor improvement[32]. Taken together, these elements suggest that striatal high gamma and beta activity may have different functional roles preferentially associated to reinforcement and sensorimotor functions, respectively.

The studies mentioned above provide associative evidence linking the presence of reinforcement with changes of neural activity within the striatum determined through neuroimaging[17,18], but do not allow to draw conclusions regarding its causal role in reinforcement motor learning in humans. The only causal evidence available to date comes from animal work showing modulation of reinforcement-based decision-making with striatal stimulation[33,34]. A reason for the current absence of investigations of the causal role of the striatum in human behaviour is related to its deep localization in the brain. As such, current non-invasive brain stimulation techniques, such as transcranial magnetic stimulation (TMS) or classical transcranial electric stimulation (tES), do not allow to selectively target deep brain regions, because these techniques exhibit a steep depth-focality trade-off[35,36]. Studies of patients with striatal lesions[37,38] or invasive deep brain stimulation of connected nuclei[39,40] have provided insights into the role of the basal ganglia in reinforcement learning. However, their conclusions are partially limited by the fact that the studied patients also exhibit altered network properties resulting from the underlying pathology (e.g., neurodegeneration, lesions) or from the respective compensatory mechanisms. Here, we address these challenges by exploiting transcranial electric Temporal Interference Stimulation (tTIS), a new non-invasive brain stimulation approach allowing to target deep brain regions in a frequency-specific and focal manner in the physiological state[41,42].

99 The concept of tTIS was initially proposed and validated on the hippocampus of rodents[41]
100 and was then further tested through computational modelling[43–47] and in first applications on
101 cortical areas in humans[48,49]. tTIS requires two pairs of electrodes to be placed on the head, each
102 pair delivering a high frequency alternating current. One key element is that this frequency has to
103 be high enough (i.e., in the kHz range) to avoid direct neuronal entrainment, based on the low-
104 pass filtering properties of neuronal membranes[50]. The second key element is the application of a
105 small difference of frequency between the two alternating currents. The superposition of the
106 electric fields creates an envelope oscillating at this low-frequency difference, which can be
107 steered towards individual deep brain structures (e.g., by optimizing electrodes' placement), and
108 is in a range able to influence neuronal activity [41,51–53]. An interesting feature of tTIS is to stimulate
109 at a particular frequency of interest in order to preferentially interact with specific neuronal
110 processes[41,42]. Importantly, despite these exciting opportunities, current evidence for tTIS-related
111 neuromodulation of deep brain structures, such as the striatum, is lacking in humans.

112 Here, we combine tTIS with electric field modelling for target localisation, behavioural data
113 and functional magnetic resonance imaging (fMRI) to evaluate the causal role of specific patterns
114 of striatal activity in reinforcement learning of motor skills. Based on the studies mentioned above,
115 we hypothesised that striatal tTIS at high gamma frequency ($tTIS_{80Hz}$) would disturb the fine-tuning
116 of high gamma oscillatory activity in the striatum and thereby would perturb reinforcement motor
117 learning in contrast to beta ($tTIS_{20Hz}$) or sham ($tTIS_{Sham}$) stimulation. More specifically, we
118 reasoned that applying a constant high gamma rhythm in the striatum would disturb the temporally
119 precise and reinforcement-specific modulation of high gamma activity. Moreover, given that the
120 stimulation protocol was not individualised to endogenous high gamma activity and not
121 synchronised to ongoing activity in other hubs of the reinforcement learning network (e.g., the
122 frontal cortex), we anticipated disruptive rather than beneficial effects of $tTIS_{80Hz}$.

In line with our prediction, we report that $tTIS_{80Hz}$ disrupted motor learning compared to the controls, but only in the presence of reinforcement. To evaluate the potential neural correlates of these behavioral effects, we measured BOLD activity in the striatum and effective connectivity between the striatum and frontal cortical areas involved in reinforcement motor learning. We found that the disruptive effect of $tTIS_{80Hz}$ on reinforcement learning was associated to a specific modulation of BOLD activity in the putamen and caudate, but not in the cortex, supporting the ability of tTIS to selectively modulate striatal activity without affecting overlying cortical areas. Moreover, $tTIS_{80Hz}$ also increased the neuromodulatory influence of the striatum on frontal cortical areas involved in reinforcement motor learning. Overall, the present study shows for the first time that tTIS can non-invasively and selectively modulate a striatal mechanism involved in reinforcement learning opening new horizons for the study of causal relationships between deep brain structures and human behaviour.

2. Results

24 healthy participants (15 women, 25.3 ± 0.1 years old; mean ± SE) performed a force tracking task in the MRI with concurrent tTIS of the striatum. The task required participants to modulate the force applied on a hand-grip force sensor in order to track a moving target with a cursor with the right, dominant hand[54,55] (**Figure 1A**). At each block, participants had to learn a new pattern of motion of the target (**Figure S1**; see Methods). In $Reinf_{ON}$ blocks, participants were provided with online reinforcement feedback during training, giving them real-time information about success or failure throughout the trial, indicated as a green or red target, respectively (please see **Video S1** for the task). The reinforcement feedback was delivered according to a closed-loop schedule[8], in which the success criterion to consider a force sample as successful was updated based on the median performance over the 4 previous trials (see Methods for more details). In $Reinf_{OFF}$ blocks, participants practiced with a visually matched random feedback (cyan/magenta). Importantly, in both types of blocks, training was performed with partial visual feedback of the cursor, a condition that has been shown to maximise reinforcement effects in various motor learning paradigms[4,56–58] and which yielded significant effects of reinforcement on motor learning as also demonstrated in an additional behavioural study testing another group of healthy participants on the same task (n = 24, Figure S2). Before and after training, participants performed Pre- and Post-training assessments with full visual feedback, no reinforcement and no tTIS, allowing us to evaluate motor learning. To assess the effect of tTIS on reinforcement-related benefits in motor learning and the associated neural changes, participants performed 6 blocks of 36 trials in the MRI, with concurrent tTIS during training, delivered with a Δf of 20 Hz ($tTIS_{20Hz}$), 80 Hz ($tTIS_{80Hz}$) or as a sham ($tTIS_{Sham}$; 3 $tTIS_{TYPE}$ x 2 $Reinf_{TYPE}$ conditions; **Figure 1B, 1C**). Notably, the order of the conditions was balanced among the 24 participants, ensuring that any potential carry-over effect would have the same impact on each experimental condition. To determine the best electrode montage to stimulate the human striatum (putamen, caudate and nucleus

accumbens [NAc] bilaterally), computational modelling with a realistic head model was conducted with Sim4Life[59] (see Methods). The selected montage (F3-F4; TP7-TP8) generated a theoretical temporal interference electric field that was ~30-40% stronger in the striatum than in the overlying cortex, reaching magnitudes of 0.5 to 0.6 V/m (**Figure 1D, 1E**).

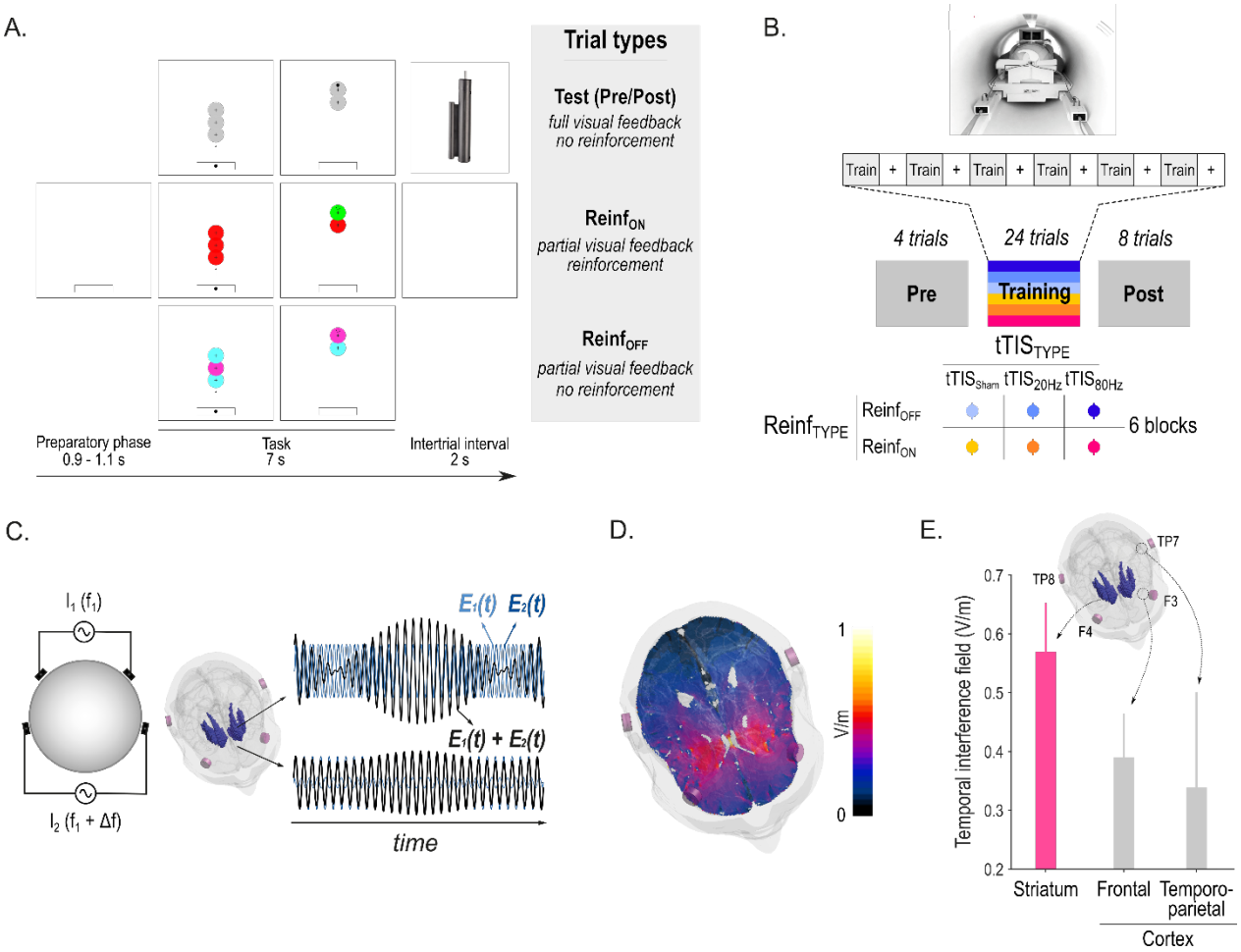

Figure 1. Striatal tTIS during reinforcement learning of motor skills in the MRI. A) Motor learning task. Participants were required to squeeze a hand grip force sensor (depicted in the upper right corner of the figure) in order to track a moving target (larger circle with a cross in the center) with a cursor (black smaller circle)[54,55]. Pre- and Post-training assessments were performed with full visual feedback of the cursor and no reinforcement. In Reinf$_{ON}$ and Reinf$_{OFF}$ trials, participants practiced the task with or without reinforcement feedback, respectively. As such, in Reinf$_{ON}$ trials, the color of the target varied in real-time as a function of the subjects' tracking performance. **B) Experimental procedure.** Participants performed the task in the MRI with concomitant TI stimulation. Blocks of training were composed of 36 trials (4 Pre-, 24 Training and 8 Post-training trials) interspersed with short resting periods (represented as + on the figure). The 6 training types resulted from the combination of 3 tTIS$_{TYPES}$ and 2 Reinf$_{TYPES}$. **C) Concept of tTIS.** On the left, two pairs of electrodes are shown on a head model and currents are applied with a

frequency f1 and f1+Δf. On the right, the interference of the two electric fields within the brain is represented for two different locations with respectively high and low envelope modulation. $E_1(t)$ and $E_2(t)$ represent the modulation of the fields' magnitude over time. tTIS was delivered either with a Δf of 20 or 80 Hz or as a sham (ramp-up and immediate ramp-down of high frequency currents with flat envelope). **D) Electric field modelling with the striatal montage.** Temporal interference exposure (electric field modulation magnitude). **E) Temporal interference exposure averaged in the striatum and in the overlying cortex.** Magnitude of the field in the cortex was extracted from the Brainnetome atlas (BNA[60]) regions underneath the stimulation electrodes (F3-F4 and TP7-TP8). Error bars represent the standard deviation over the voxels in the considered region.

$tTIS_{80Hz}$ disrupts reinforcement learning of motor skills

Task performance was evaluated by means of the Error, which was defined as the absolute difference between the applied and target force averaged across samples for each trial, as done previously[4,54,56] (**Figure 2A**). Across conditions, the Post-training Error was reduced compared to the Pre-training Error (single sample t-test on the normalised Post-training data: $t_{(24)}$=-2.69; p=0.013; Cohen's d=-0.55), indicating significant motor learning during the task (**Figure 2B**). Such improvement was greater when participants had trained with reinforcement ($Reinf_{TYPE}$ effect in the Linear Mixed Model (LMM): $F_{(1,\ 1062.2)}$=5.17; p=0.023; d=-0.14 for the post-hoc contrast $Reinf_{ON}$ – $Reinf_{OFF}$), confirming the beneficial effect of reinforcement on motor learning[7,58]. Crucially though, this effect depended on the type of stimulation applied during training ($Reinf_{TYPE}$ x $tTIS_{TYPE}$ interaction: $F_{(2,\ 1063.5)}$=2.11; p=0.034; **Figure 2C**). While reinforcement significantly improved learning when training was performed with $tTIS_{Sham}$ (p=0.036; d=-0.22) and $tTIS_{20Hz}$ (p=0.0089; d=-0.27), this was not the case with $tTIS_{80Hz}$ (p=0.43; d=0.083). Consistently, direct between-condition comparisons showed that in the $Reinf_{ON}$ condition, learning was reduced with $tTIS_{80Hz}$ compared to $tTIS_{20Hz}$ (p=0.039; d=0.26) and $tTIS_{Sham}$ (p<0.001; d=0.45) but was not different between $tTIS_{20Hz}$ and $tTIS_{Sham}$ (p=0.15; d=0.20). This disruption of motor learning with $tTIS_{80Hz}$ was not observed in the absence of reinforcement ($tTIS_{80Hz}$ vs. $tTIS_{20Hz}$: p=0.59; d=-0.10, $tTIS_{80Hz}$ vs. $tTIS_{Sham}$: p=0.34; d=0.15). These results strongly point to the fact that high gamma striatal tTIS

207 specifically disrupts the benefits of reinforcement on motor learning and not motor learning in
208 general.

209 Although training with $tTIS_{20Hz}$ did not alter the benefits of reinforcement on motor learning,
210 we found that learning without reinforcement was significantly impaired in this condition ($tTIS_{20Hz}$
211 vs. $tTIS_{Sham}$: p=0.046; d=0.25, **Figure 2C**). This suggests that $tTIS_{20Hz}$ may disrupt a qualitatively
212 different mechanism involved in motor learning from sensory feedback[61], in line with the role of
213 striatal beta oscillations in sensorimotor function[28].

214 Next, we evaluated the effect of tTIS on motor performance during training itself. As shown
215 in Figure 2A, the Error was generally higher during Training than in Test trials due to the presence
216 of visual uncertainty during this phase. The extent of this disruption was reduced in the presence
217 of reinforcement ($Reinf_{TYPE}$: $F_{(1,\ 3262.4)}$=339.89; p<0.001; d=-0.64 for the contrast $Reinf_{ON}$ –
218 $Reinf_{OFF}$), demonstrating the ability of subjects to exploit real-time reinforcement information to
219 improve tracking (**Figure 2D**). Notably, this effect was not modulated by $tTIS_{TYPE}$ ($Reinf_{TYPE}$ x
220 $tTIS_{TYPE}$: $F_{(2,\ 3265.8)}$=0.91; p=0.40), indicating that tTIS did not directly influence reinforcement gains
221 during tracking. Interestingly though, striatal stimulation did impact on general tracking
222 performance independently of reinforcement as indicated by a significant $tTIS_{TYPE}$ effect ($tTIS_{TYPE}$:
223 $F_{(2,\ 3262.4)}$=42.85; p<0.001). This effect was due to an increase in the Error when $tTIS_{20Hz}$ was
224 applied (p<0.001; d=0.28 when compared to $tTIS_{Sham}$), which was even stronger during $tTIS_{80Hz}$
225 (p<0.001; d=0.38 and p=0.031; d=0.11 when compared to $tTIS_{Sham}$ and $tTIS_{20Hz}$, respectively). An
226 additional analysis showed that the detrimental effect of tTIS on motor performance was actually
227 due to an impaired ability to improve performance during Training (LMM with continuous fixed
228 effect Trial: $tTIS_{TYPE}$ x Trial interaction: $F_{(2,\ 3399)}$=4.46; p=0.012, post-hoc tests: $tTIS_{Sham}$ vs. $tTIS_{20Hz}$:
229 p=0.013; $tTIS_{Sham}$ vs. $tTIS_{80Hz}$: p=0.068; $tTIS_{20Hz}$ vs. $tTIS_{80Hz}$: p=0.81; **Figure S3**). However, again,
230 this effect did not depend on the presence of reinforcement ($Reinf_{TYPE}$ x $tTIS_{TYPE}$ x Trial: $F_{(2,}$
231 $_{3399)}$=0.51; p=0.60). Notably, we also found that the detrimental effect of striatal tTIS did not depend

232 on the availability of visual information on the cursor, but rather that tTIS had a general effect on
233 motor performance irrespective of visual and reinforcement feedback (see Supplementary
234 materials). This analysis also confirmed that reinforcement gains in motor performance were
235 stronger when visual information was not available (**Figure S4**), in line with the behavioural data
236 mentioned above (Figure S2) and previous studies[57,62]. Overall, these results suggest that striatal
237 tTIS altered motor performance in a frequency-dependent manner but did not influence the ability
238 to rapidly adjust motor commands based on reinforcement feedback during training. Hence,
239 $tTIS_{80Hz}$ may not disrupt real-time processing of reinforcement feedback, but may rather impair the
240 beneficial effect of reinforcements on the retention of motor memories[6,7].

241 Notably, these effects could not be explained by potential differences in initial performance
242 between conditions ($Reinf_{TYPE}$ x $tTIS_{TYPE}$: $F_{(2, 519.99)}$=1.08; p=0.34), nor by changes in the flashing
243 properties of the reinforcement feedback (i.e., the frequency of color change during tracking;
244 $Reinf_{TYPE}$ x $tTIS_{TYPE}$: $F_{(2, 3283)}$=0.19; p=0.82), or by differences in success rate in the $Reinf_{ON}$ blocks
245 (i.e., the proportion of success feedback during tracking; $tTIS_{TYPE}$: $F_{(2, 1702)}$=0.17; p=0.84). The
246 $Reinf_{TYPE}$ x $tTIS_{TYPE}$ effect on learning was also not influenced by the order of the reinforcement
247 conditions (analysis on sub-groups based on whether participants experienced $Reinf_{ON}$ or $Reinf_{OFF}$
248 first; no $Reinf_{TYPE}$ x $tTIS_{TYPE}$ x $Group_{TYPE}$ interaction: $F_{(2,1105.06)}$=1.75; p=0.17; see Supplementary
249 materials for more details on these analyses).

250 Finally, we confirmed that these results were not a consequence of an inefficient blinding.
251 As such, when debriefing after the experiment, only 6/24 participants were able to successfully
252 identify the order of the stimulation applied (e.g., real – real – placebo; chance level: 4/24; Fisher
253 exact test on proportions: p=0.74). Consistently, the magnitude (**Figure S5A**) and type (**Figure**
254 **S5B**) of tTIS-evoked sensations evaluated before the experiment were qualitatively similar across
255 conditions and tTIS was generally well tolerated in all participants (no adverse events reported).
256 This suggests that blinding was successful and is unlikely to explain our findings. More generally,

this is a first indication that tTIS evokes very limited sensations (e.g., only 2/24 and 1/24 subjects rated sensations evoked at 2 mA as "strong" for $tTIS_{20Hz}$ and $tTIS_{80Hz}$, respectively; **Figure S5A**) that are compatible with efficient blinding.

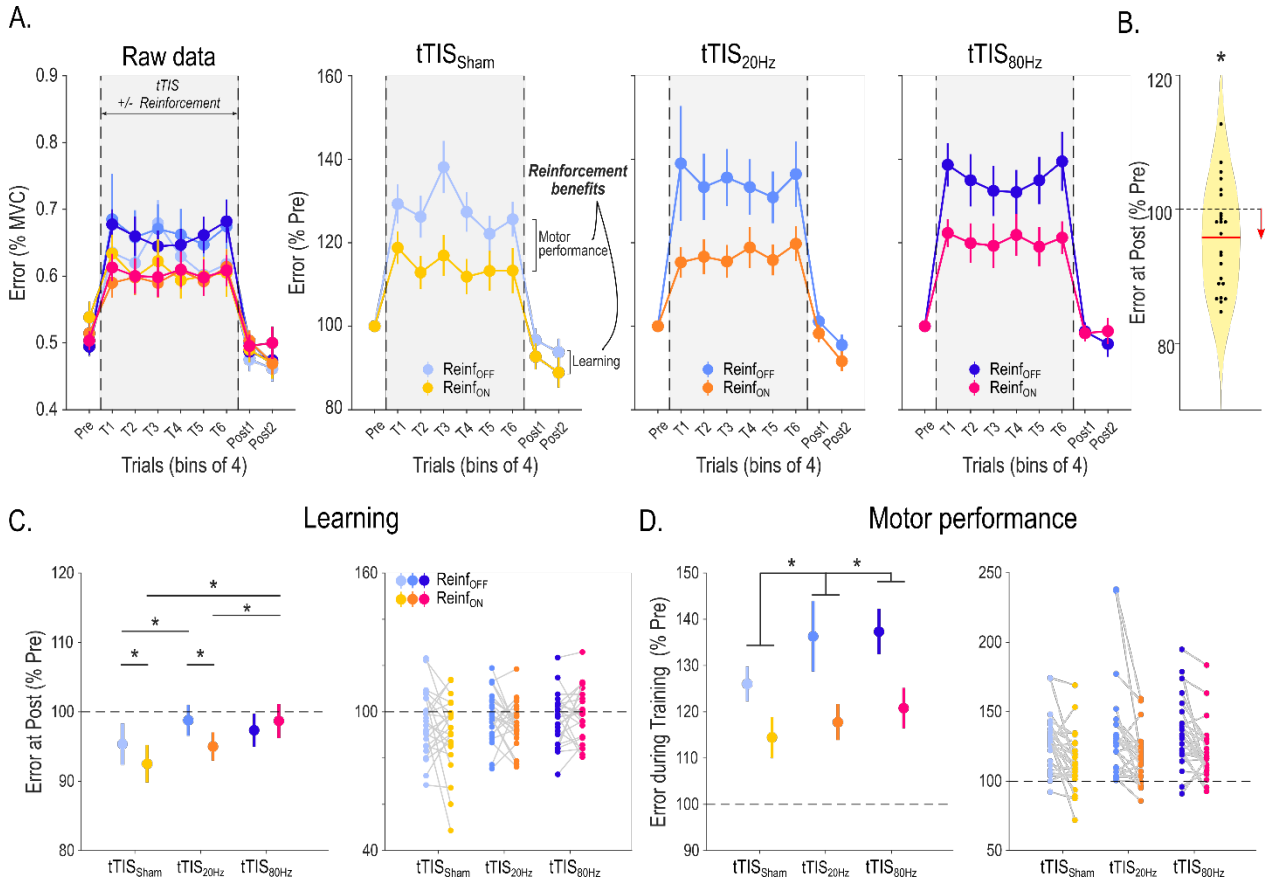

Figure 2. Behavioural results. A) Motor performance across training. Raw Error data (expressed in % of Maximum Voluntary Contraction [MVC]) are presented on the left panel for the different experimental conditions in bins of 4 trials. The increase in Error during Training is related to the visual uncertainty (i.e., intermittent disappearance of the cursor) that was applied to enhance reinforcement effects. On the right, the three plots represent the Pre-training normalised Error in the $tTIS_{Sham}$, $tTIS_{20Hz}$ and $tTIS_{80Hz}$ blocks. Reinforcement-related benefits represent the improvement in the Error measured in the $Reinf_{ON}$ and $Reinf_{OFF}$ blocks, during Training (reflecting benefits in motor performance) or at Post-training (reflecting benefits in learning). **B) Averaged learning across conditions.** Violin plot showing the Error distribution at Post-training (expressed in % of Pre-training) averaged across conditions, as well as individual subject data. A single-sample t-test showed that the Post-training Error was reduced compared to the Pre-training level, indicating significant learning in the task. **C) Motor learning.** Averaged Error at Post-training (normalised to Pre-training) and the corresponding individual data points in the different experimental conditions are shown on the left and right panels, respectively, for the subjects included in the analysis (i.e., after outlier detection, remaining n=23). Reduction of Error at Post-training reflects true improvement at tracking the target in Test conditions (in the absence of reinforcement, visual uncertainty or tTIS). The LMM ran on these data revealed a specific effect

of $tTIS_{80Hz}$ on reinforcement-related benefits in learning. **D) Motor performance.** Averaged Error during Training (normalised to Pre-training) and the corresponding individual data points in the different experimental conditions are shown on the left and right panels, respectively, for the subjects included in the analysis (i.e., after outlier detection, n=23). Individual data points are shown on the right panel. Error change during Training reflect the joint contribution of the experimental manipulations (visual uncertainty, potential reinforcement and tTIS) on motor performance. The LMM ran on these data showed a frequency-dependent effect of tTIS on motor performance, irrespective of reinforcement. *: $p<0.05$. Data are represented as mean ± SE.

The effect of $tTIS_{80Hz}$ on reinforcement motor learning is related to modulation of neural activity in the striatum

As mentioned above, task-based fMRI was acquired during Training with concomitant tTIS. This allowed us to evaluate the neural effects of tTIS and their potential relationship to the behavioural effects reported above. As a first qualitative evaluation of the data, we performed a whole-brain analysis in the $tTIS_{Sham}$ condition to assess the network activated during reinforcement motor learning ($Reinf_{ON}$ condition). Consistent with previous neuroimaging studies employing similar tasks[63,64], we found prominent BOLD activations in a motor network including the putamen, thalamus, cerebellum and sensorimotor cortex, particularly on the left hemisphere, contralateral to the trained hand (**Figure S6, Table S2**). Notably though, contrasting $Reinf_{ON}$ and $Reinf_{OFF}$ conditions did not reveal any significant cluster at the whole-brain level. Hence, this first analysis did not reveal any region specifically activated in the presence of reinforcement, but rather confirms the involvement of a motor network engaged in this type of task irrespective of the reinforcement feedback.

As a second step, we evaluated the effect of tTIS on striatal activity, as a function of the type of reinforcement feedback and focusing on the very same regions of interest (ROI) that were used to optimise tTIS exposure in the modelling. Based on this, we extracted averaged BOLD activity within the bilateral putamen, caudate and NAc based on the Brainnetome atlas (BNA[60]), in the different experimental conditions and considered these six striatal ROIs (ROI_{STR}) as fixed effects in the LMM. This model revealed a strong enhancement of striatal activity with $Reinf_{ON}$ with

respect to $Reinf_{OFF}$ ($F_{(1,\ 800.01)}$=13.23; p<0.001; d=0.25 for the contrast $Reinf_{ON}$ – $Reinf_{OFF}$) consistent with previous literature[11], but no $tTIS_{TYPE}$ effect ($F_{(2,\ 800.01)}$=0.46; p=0.63) and no interaction (all p> 0.65; **Figure 3A**). Despite the absence of effects of tTIS on averaged striatal activity, we then asked whether the behavioural effects of $tTIS_{80Hz}$ on reinforcement motor learning (i.e., $tTIS_{80Hz}$ vs. $tTIS_{20Hz}$ and $tTIS_{Sham}$ with $Reinf_{ON}$) could be linked to modulation of activity in core brain regions. To do so, we ran a whole-brain analysis focusing on the main behavioural effects mentioned above. Results revealed that the effect of $tTIS_{80Hz}$ (with respect to $tTIS_{20Hz}$) on motor learning in the $Reinf_{ON}$ condition was specifically related to modulation of activity in two clusters encompassing the left putamen and bilateral caudate (**Figure 3B, Table S3**). Notably, the presence of the high frequency carrier (kHz) in both stimulation conditions rules out the possibility that the correlation was due to putative neuromodulatory effects of high frequency stimulation. No significant clusters were found neither for the $tTIS_{80Hz}$ – $tTIS_{Sham}$ contrast, nor for the control $tTIS_{20Hz}$ - $tTIS_{Sham}$ contrast, indicating that the reported correlation is not due to a general link between striatal activity and reinforcement motor learning. Overall, these results provide evidence that the detrimental effect of $tTIS_{80Hz}$ on reinforcement learning of motor skills is related to modulation of neural activity specifically in the striatum.

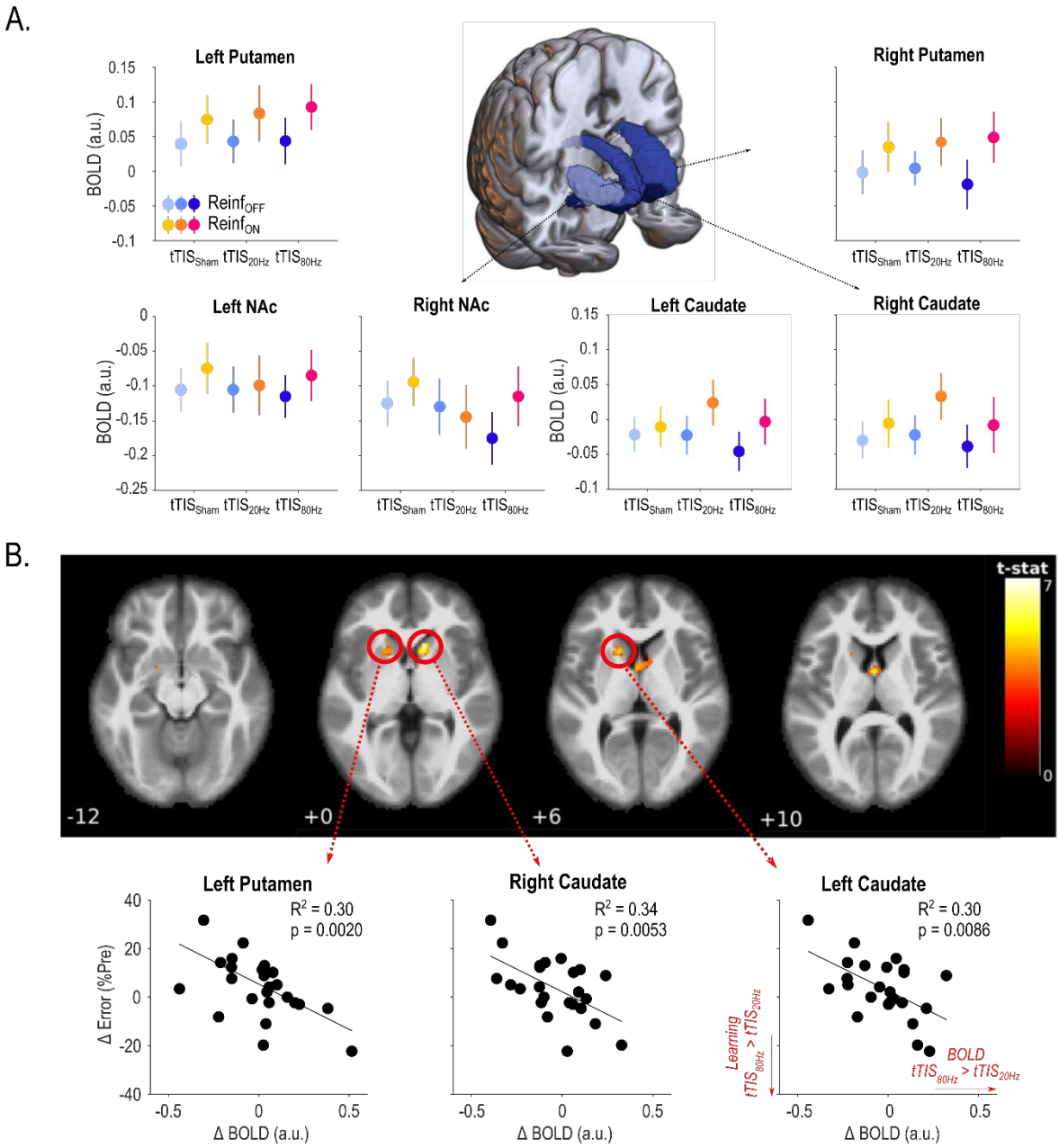

Figure 3. Striatal activity. A) Striatal BOLD responses. A 3D-reconstruction of the striatal masks used in the current experiment is surrounded by plots showing averaged BOLD activity for each mask in the different experimental conditions. A LMM ran on these data showed higher striatal responses in the $Reinf_{ON}$ with respect to the $Reinf_{OFF}$ condition, but no effect of $tTIS_{TYPE}$ and no interaction. **B) Whole-brain activity associated to the behavioural effect of $tTIS_{80Hz}$ on reinforcement motor learning.** Correlation between tTIS-related modulation of striatal activity ($tTIS_{80Hz}$ – $tTIS_{20Hz}$) and learning abilities in the $Reinf_{ON}$ condition. Significant clusters of correlation were found in the left putamen and bilateral caudate (uncorrected voxel-wise FWE: p=0.001, and corrected cluster-based FDR: p=0.05). Lower panel shows individual correlations for the three significant regions highlighted in the whole-brain analysis. *: p<0.05. Data are represented as mean ± SE.

336 **$tTIS_{80Hz}$ enhances effective connectivity between the striatum and frontal cortex.**

337 Interactions between the striatum and frontal cortex are crucial for a variety of behaviours
338 including motor and reinforcement learning[13]. In particular, reinforcement motor learning requires
339 to use information about task success to guide future motor commands[4], a process for which the
340 striatum may play an integrative role at the interface between fronto-striatal loops involved in
341 reward processing and motor control[13,65]. In a subsequent analysis, we asked whether striatal tTIS
342 modulates striatum to frontal cortex communication during reinforcement motor learning. More
343 specifically, we computed effective connectivity (using the generalized psychophysiological
344 interactions method[66]) between striatal and frontal regions classically associated with motor and
345 reward-related functions, and thought to be involved in reinforcement motor learning[67,68]. For the
346 motor network, we evaluated effective connectivity between motor parts of the striatum (i.e., dorso-
347 lateral putamen (dlPu) and dorsal caudate (dCa)) and two regions strongly implicated in motor
348 learning: the medial part of the supplementary motor area (SMA) and the part of the primary motor
349 cortex (M1) associated to upper limb functions (**Figure 4A**). For the reward network, we assessed
350 connectivity between parts of the striatum classically associated to limbic functions (i.e., the NAc
351 and the ventro-medial putamen (vmPu) and two frontal areas involved in reward processing: the
352 anterior cingulate cortex (ACC) and the ventro-medial prefrontal cortex (vmPFC; **Figure 4B**; [11]).
353 The LMM ran with the fixed effects $Reinf_{TYPE}$, $tTIS_{TYPE}$ and $Network_{TYPE}$ showed a significant effect
354 of $tTIS_{TYPE}$ ($F_{(2, 2264.0)}$=5.42; p=0.0045), that was due to higher connectivity in the $tTIS_{80Hz}$ condition
355 with respect to $tTIS_{Sham}$ (p=0.0038; d=0.16) and $tTIS_{20Hz}$ (at the trend level, p=0.069; d=0.11). There
356 was no difference in connectivity between $tTIS_{20Hz}$ and $tTIS_{Sham}$ (p=0.58; d=0.051). Hence, $tTIS_{80Hz}$,
357 but not $tTIS_{20Hz}$, enhanced effective connectivity between the striatum and frontal cortex during
358 motor training. This increase in effective connectivity with $tTIS_{80Hz}$ actually led to a connectivity
359 closer to the resting state (values closer to 0, see Methods). Put differently, while the task induced

360 a reduction in effective connectivity between striatum and frontal cortex, $tTIS_{80Hz}$ disrupted this
361 modulation by bringing connectivity back to the resting state.

362 The LMM did not reveal any effect of $Reinf_{TYPE}$ ($F_{(1, 2264.0)}$=0.010; p=0.92), $Network_{TYPE}$ ($F_{(1,}$
363 $_{2264.0)}$=3.16; p=0.076) and no double interaction (note the trend for a $Reinf_{TYPE}$ x $Network_{TYPE}$ effect
364 though: $F_{(1, 2264.0)}$=3.52; p=0.061). Yet, we did find a significant $Reinf_{TYPE}$ x $tTIS_{TYPE}$ x $Network_{TYPE}$
365 interaction ($F_{(2, 2264.0)}$=4.87; p=0.0078). Such triple interaction was related to the fact that $tTIS_{80Hz}$
366 increased connectivity in the $Reinf_{ON}$ condition in the motor network ($Reinf_{ON}$ vs. $Reinf_{OFF}$:
367 p=0.0012; d=0.33; Figure 4A), while it tended to have the opposite effect in the reward network
368 (p=0.063; d=-0.19; Figure 4B). This increase was not present in any of the two networks when
369 either $tTIS_{Sham}$ or $tTIS_{20Hz}$ were applied (all p> 0.40). Moreover, in the motor network, connectivity
370 in the $Reinf_{ON}$ condition was higher with $tTIS_{80Hz}$ than with $tTIS_{Sham}$ (p<0.001; d=0.42) and $tTIS_{20Hz}$
371 (at the trend level; p=0.059; d=0.23, Figure 4A). These data suggest that $tTIS_{80Hz}$ enhanced the
372 neuromodulatory influence of the striatum on motor cortex during task performance, but only in
373 the presence of reinforcement. In the reward network, post-hocs revealed that connectivity in the
374 $Reinf_{OFF}$ condition was significantly higher with $tTIS_{80Hz}$ compared to $tTIS_{20Hz}$ (p=0.045; d=0.25;
375 Figure 4B), in line with the general effect of $tTIS_{TYPE}$ on connectivity reported above. This pattern
376 of results suggests that the increase of connectivity from striatum to frontal cortex observed with
377 $tTIS_{80Hz}$ depends on the presence of reinforcement, in particular in the motor network. Such
378 reinforcement-dependent increase of connectivity may reflect the preferential effect of $tTIS_{80Hz}$ on
379 striatal gamma oscillations[69] in a situation where these oscillations are already boosted by the
380 presence of reinforcement[19] (see Discussion).

381 In a subsequent analysis, we verified that these results did not depend on the specific
382 frontal ROIs considered in the analysis (ROI_{TYPE}: M1 and SMA in the motor network and ACC and
383 vmPFC in the reward network). Importantly, we did not find a $tTIS_{TYPE}$ x $Reinf_{TYPE}$ x ROI_{TYPE}
384 interaction neither in the motor ($F_{(2,1112)}$=0.83; p=0.44) nor in the reward network ($F_{(2,1112)}$=0.61;

p=0.54), suggesting that the main connectivity results were consistent within a network and were not influenced by the specific frontal ROI included in the analysis (see Supplementary materials for more details on this analysis). As an additional control, we verified that the effects of $tTIS_{TYPE}$ on connectivity could not be observed in a control network associated to language (as defined by [70]), which was unlikely to be involved in the present task and did not include the striatum (see Methods). As expected, effective connectivity within the language network was not modulated by $Reinf_{TYPE}$ ($F_{(1, 547)}$=0.81; p=0.37), nor by $tTIS_{TYPE}$ ($F_{(2, 547)}$=0.58; p=0.56), or by $Reinf_{TYPE}$ x $tTIS_{TYPE}$ ($F_{(2, 547)}$=0.45; p=0.64). Hence, tTIS and reinforcement-related changes in connectivity were consistent within the considered fronto-striatal networks and not observed in a control network unrelated to the task.

Notably, contrary to the BOLD results presented above, we did not find any correlations between the effects of $tTIS_{80Hz}$ on connectivity and motor learning, neither in the motor (robust linear regression: $tTIS_{80Hz}$ – $tTIS_{Sham}$: R^2=0.019; p=0.48; $tTIS_{80Hz}$ – $tTIS_{20Hz}$: R^2=0.034; p=0.54) nor in the reward ($tTIS_{80Hz}$ – $tTIS_{Sham}$: R^2=0.037; p=0.46; $tTIS_{80Hz}$ – $tTIS_{20Hz}$: R^2<0.001; p=0.75) network, suggesting some degree of independence between the effect of $tTIS_{80Hz}$ on reinforcement motor learning and on effective connectivity.

Overall, these results highlight the ability of $tTIS_{80Hz}$, but not $tTIS_{20Hz}$, to modulate striatum to frontal cortex connectivity, depending on the presence of reinforcement. However, the absence of correlation with the behaviour suggests that this effect may not be directly associated to the detrimental effect of $tTIS_{80Hz}$ on reinforcement motor learning or that $tTIS_{80Hz}$-related changes in striato-frontal communication were linked to other aspects of reinforcement learning not captured by our task.

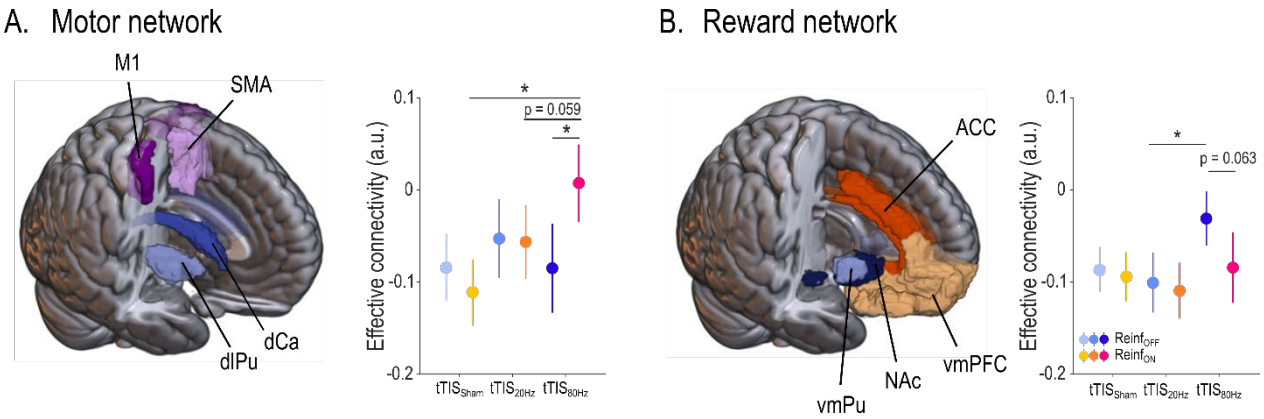

Figure 4. Striatum to frontal cortex effective connectivity. A) Motor network. On the left, 3D reconstruction of the masks used for the motor network (i.e., dorso-lateral putamen, dorsal caudate, M1, SMA). On the right, plot showing effective connectivity from motor striatum to motor cortex in the different experimental conditions. Note the increase of connectivity with $tTIS_{80Hz}$ in the presence of reinforcement. **B) Reward network.** On the left, 3D reconstruction of the masks used for the reward network (i.e., ventro-medial putamen, NAc, vmPFC, ACC). On the right, plot showing effective connectivity from motor striatum to motor cortex in the different experimental conditions. ROIs were defined based on the BNA atlas[12] *: $p<0.05$. Data are represented as mean ± SE.

418 **Neural effects of $tTIS_{80Hz}$ depend on impulsivity**

419 Determining individual factors that shape responsiveness to non-invasive brain stimulation
420 approaches is a crucial step to better understand the mechanisms of action but also to envision
421 stratification of patients in future clinical interventions[71]. A potential factor that could explain inter-
422 individual differences in responsiveness to $tTIS_{80Hz}$ is the level of impulsivity. As such, impulsivity
423 has been associated to changes of gamma oscillatory activity in the striatum of rats[72] and to the
424 activity of fast-spiking interneurons in the striatum[73,74], a neuronal population that is strongly
425 entrained to gamma rythms[19,21] and may therefore be particularly sensitive to $tTIS_{80Hz}$. In a
426 subsequent exploratory analysis, we asked if the neural effects of $tTIS_{80Hz}$ were associated to
427 impulsivity levels, as evaluated by a well-established independent delay-discounting questionnaire
428 performed at the beginning of the experiment[75,76]. Strikingly, a whole-brain analysis revealed that
429 impulsivity was associated to the effect of $tTIS_{80Hz}$ on BOLD activity (with respect to $tTIS_{20Hz}$)
430 specifically in the left caudate nucleus (**Figure S7A, S7B, Table S4**). Moreover, the effect of
431 $tTIS_{80Hz}$ on striatum to motor cortex connectivity reported above was negatively correlated to
432 impulsivity both when contrasting $tTIS_{80Hz}$ with $tTIS_{Sham}$ (**Figure S7C, left**) and with $tTIS_{20Hz}$ (**Figure**
433 **S7C, middle**). Such correlations were absent when contrasting $tTIS_{20Hz}$ with $tTIS_{Sham}$ (**Figure S7C,**
434 **right**), as well as when considering the same contrasts in the reward instead of the motor network
435 (see Supplementary materials for more details). Taken together, these results suggest that inter-
436 individual variability in impulsivity might influence the neural responses to striatal $tTIS_{80Hz}$.

3. Discussion

In this study, we combined striatal tTIS with electric field modelling, behavioural and fMRI analyses to evaluate the causal role of the striatum in reinforcement learning of motor skills in healthy humans. $tTIS_{80Hz}$, but not $tTIS_{20Hz}$, disrupted the ability to learn from reinforcement feedback. This behavioural effect was associated to modulation of neural activity specifically in the striatum. As a second step, we show that $tTIS_{80Hz}$, but not $tTIS_{20Hz}$, increased the neuromodulatory influence of the striatum on connected frontal cortical areas involved in reinforcement motor learning. Finally, inter-individual variability in the neural effects of $tTIS_{80Hz}$ could be partially explained by impulsivity, suggesting that this trait may constitute a determinant of responsiveness to high gamma striatal tTIS. Overall, the present study shows for the first time that striatal tTIS can non-invasively modulate a striatal mechanism involved in reinforcement learning, opening new horizons for the study of causal relationships between deep brain structures and human behaviour.

We investigated the causal role of the human striatum in reinforcement learning of motor skills in healthy humans; a question that cannot be addressed with conventional non-invasive brain stimulation techniques. In particular, by stimulating at different frequencies, we aimed at dissociating striatal mechanisms involved in reinforcement and sensorimotor learning. In line with our main hypothesis, we found that striatal $tTIS_{80Hz}$ altered reinforcement learning of a motor skill. Such disruption was frequency- and reinforcement-specific: learning was not altered with striatal $tTIS_{20Hz}$ in the presence of reinforcement, or when striatal $tTIS_{80Hz}$ was delivered in the absence of reinforcement. The rationale to stimulate at high gamma frequency was based on previous work showing reinforcement-related modulation of gamma oscillations in the striatum[19–21,24,26,72,77] and in the frontal cortex[77–80]. Several neuronal mechanisms may contribute to the detrimental effect of $tTIS_{80Hz}$ on reinforcement motor learning. First, as $tTIS_{80Hz}$ consisted in a constant high gamma

oscillating field applied on the striatum, it may have perturbed the encoding of reinforcement information into high gamma oscillations[19–21,25–27], preventing participants to learn the motor skill based on different outcomes. Put differently, $tTIS_{80Hz}$ may specifically saturate high gamma activity in the striatum preventing reinforcement-related modulations[81]. Moreover, because reinforcement motor learning likely engages synchronised activity in a network of regions including fronto-striatal loops, neuromodulation of a single node of the circuit may alter synchronisation of activity in the network[81] and the temporal coordination with interacting rhythms[25]. Finally, because we did not have access to electrophysiological recordings of oscillatory activity in the striatum, the applied stimulation was not personalised as it did not take into account the individual high gamma frequency peak associated to reward processing and the potential heterogeneity of gamma activity within the striatum[24]. Hence, $tTIS_{80Hz}$ may have resulted in a frequency mismatch between the endogenous high gamma activity and the externally imposed rhythm, that could paradoxically result in a reduction of neuronal entrainment, in particular when the frequency mismatch is relatively low[82]. Importantly, in contrast to striatal $tTIS_{80Hz}$, we found that $tTIS_{20Hz}$ reduced learning, but only in the absence of reinforcement. This result fits well with the literature linking striatal beta oscillations to sensorimotor functions[28,29,31,83–85]. Taken together, an interpretation of these results is that different oscillations within the striatum support qualitatively distinct motor learning mechanisms with beta activity contributing mostly to sensory-based learning and high gamma activity being particularly important for reinforcement learning. This being said, it is important to note that because we do not have concurrent electrophysiological recordings within the striatum, we cannot be sure that the effects of $tTIS_{20Hz}$ and $tTIS_{80Hz}$ were related to frequency-specific interactions with beta or high gamma rhythms respectively, or rather resulted from different broadband responses when stimulating at these frequencies. Yet, these results still suggest that sensory- and reinforcement-based motor learning rely on partially different neural mechanisms, in line with previous literature[8,9,61,68,86,87].

487 Interestingly, striatal tTIS also impaired tracking performance during training, irrespective
488 of the presence of reinforcement. This frequency-dependent reduction of motor performance may
489 be due to altered neuronal processing in the sensorimotor striatum that may lead to less fine-tuned
490 motor control abilities[88]. Importantly though, tTIS did not modulate the ability of participants to
491 benefit from real-time reinforcement feedback during motor performance. This suggests that
492 striatal $tTIS_{80Hz}$ altered the beneficial effects of reinforcement on learning (as evaluated in Test
493 conditions at Post-training), but not on motor performance (as evaluated during Training). Such
494 dissociation between the effects of striatal $tTIS_{80Hz}$ on reinforcement-related gains in motor
495 performance and learning may be explained by the fact that these two phases of the protocol
496 probe different processes[7,54,56,89–91]. While improvement of motor performance with reinforcement
497 relies on rapid feedback corrections based on expected outcomes[67,92–95], reinforcement gains in
498 learning (i.e., probed in Test conditions without reinforcement) may rather reflect the beneficial
499 effect of reinforcement on the retention of motor memories[5,7,54,90]. This idea that mechanisms
500 underlying performance changes in training and retention phases are partially different is well
501 supported by previous motor learning literature[6,8,96]. For instance, in sensorimotor adaptation
502 paradigms, the presence of reward boosts motor memory retention but not the adaptation process
503 itself[7,97], and M1 transcranial direct current stimulation modulates the effect of reward on retention
504 but has no effect on the training phase[90]. Hence, a potential explanation for the present results is
505 that striatal $tTIS_{80Hz}$ did not disrupt rapid motor corrections based on recent outcomes during
506 training, but may rather alter the strengthening of the memory trace based on reinforcements[6,7].
507 Overall, these results are compatible with the view that specific patterns of oscillatory activity in
508 the striatum are involved in motor control and learning processes[31], and can be modulated with
509 electrical stimulation[69,98,99].

510 To better understand the neural effects and frequency-specificity of tTIS, we coupled
511 striatal tTIS and task performance with simultaneous fMRI acquisition. The imaging results support

512 the view that the effect of $tTIS_{80Hz}$ on reinforcement learning of motor skills was indeed related to
513 neuromodulation of the striatum. As such, when considering averaged BOLD activity, we found a
514 general increase of striatal activity when reinforcement was provided[11], but no effect of tTIS.
515 Crucially though, the detrimental effect of $tTIS_{80Hz}$ on reinforcement learning was related to a
516 specific modulation of activity in the caudate and putamen, providing evidence that the present
517 behavioural effects were indeed driven by focal neuromodulation of the striatum (Figure 3).
518 Interestingly, participants with stronger disruption of reinforcement learning at the behavioural
519 level were also the ones exhibiting stronger suppression of striatal activity with $tTIS_{80Hz}$ (compared
520 to $tTIS_{20Hz}$), suggesting that tTIS-induced reduction of striatal activity is detrimental for
521 reinforcement motor learning. Further analyses showed that $tTIS_{80Hz}$, but not $tTIS_{20Hz}$, increased
522 the neuromodulatory influence of the striatum on frontal areas known to be important for motor
523 learning and reinforcement processing[96,100]. More specifically, $tTIS_{80Hz}$ disrupted the task-related
524 decrease in connectivity observed with $tTIS_{Sham}$ and $tTIS_{20Hz}$, bringing connectivity closer to
525 resting-state values. Interestingly, this effect depended on the type of network considered (reward
526 vs. motor) and on the presence of reinforcement. Striatal $tTIS_{80Hz}$ coupled with reinforcement
527 increased connectivity between the motor striatum and the motor cortex while it tended to have
528 the opposite effect when considering the connectivity between limbic parts of the striatum and pre-
529 frontal areas involved in reward processing (Figure 4). This result may reflect the differential
530 influence of striatal tTIS on distinct subparts of the striatum, depending on their pattern of activity
531 during the task[52]. As such, a recent study in non-human primates showed that tACS can have
532 opposite effects on neuronal activity based on the initial entrainment of neurons to the target
533 frequency[82]. Hence, the present differential effects of $tTIS_{80Hz}$ on motor and reward striato-frontal
534 pathways may be due to different initial patterns of activity in these networks in the presence of
535 reinforcement. Electrophysiological recordings with higher temporal resolution than fMRI are
536 required to confirm or infirm this hypothesis. Overall, the present neuroimaging results support the

537 idea that the behavioural effects of striatal $tTIS_{80Hz}$ on reinforcement learning are associated to a
538 selective modulation of striatal activity that influences striato-frontal communication.

539 The fact that we observed increased connectivity with $tTIS_{80Hz}$ and at the same time a
540 disruption of behaviour may appear contradictory at first glance. Yet, multiple lines of evidence
541 indicate that increases in connectivity are not necessarily beneficial for behaviour. For instance,
542 the severity of motor symptoms in Parkinson's disease is associated with excessive connectivity
543 in the beta band and reduction of such connectivity with treatment is associated to clinical
544 improvement[29,32]. Moreover, there is evidence that excessive functional[101,102] as well as
545 structural[103,104] connectivity in fronto-striatal circuits is associated to impulsivity. Hence, the
546 increase in connectivity observed with $tTIS_{80Hz}$ appears to be compatible with the behavioural
547 findings. This being said, contrary to the BOLD results, we did not find any correlation between
548 the effects of $tTIS_{80Hz}$ on connectivity and on reinforcement motor learning, suggesting some
549 degree of independence between these two effects. Future studies could aim at determining if
550 $tTIS_{80Hz}$-related changes in striato-frontal communication are linked to other aspects of reward
551 processing, not captured by our reinforcement motor learning task.

552 From a methodological point of view, the present results provide new experimental support
553 to the idea that the effects of tTIS are related to amplitude modulation of electric fields deep in the
554 brain and not to the high frequency fields themselves, in line with recent work[41,42,52]. As such, the
555 different behavioural and neural effects of striatal $tTIS_{80Hz}$ and $tTIS_{20Hz}$ despite comparable carrier
556 frequencies (centered on 2kHz) indicate that temporal interference was indeed the driving force
557 of the present effects. Moreover, disruption of reinforcement motor learning with $tTIS_{80Hz}$ (relative
558 to $tTIS_{20Hz}$) was specifically related to neuromodulation of the striatum, where the amplitude of the
559 tTIS field was highest according to our simulations (see [51,53] for recent validations of comparable
560 simulations in cadavers experiments). Hence, we believe that the frequency- and reinforcement-
561 dependent tTIS effects reported here cannot be explained by direct modulation of neural activity

562 by the high frequency fields. Yet, disentangling the neural effects of the low-frequency envelope
563 and the high frequency carrier appears as an important next step to better characterise the
564 mechanisms underlying tTIS[47]. We also note that the tTIS field strengths achieved according to
565 our simulations (in the range of 0.5-0.6 V/m) were sufficient to induce behavioral and neural
566 effects, in line with recent data[52,53] (see also [48]). Determining the minimum effective dose for tTIS
567 is an important line of future research given recent simulation results suggesting that stimulation
568 via an amplitude modulation with high frequency carrier signals (such as arising during tTIS) may
569 require higher dosages compared to conventional electrical stimulation with low frequencies (such
570 as during tACS), likely due to the low-pass filtering properties of neurons[43,105].

571 Finally, the strength of the behavioural effects of tTIS can be considered small to medium[106]
572 (d=0.2-0.5). We note that these effect sizes are consistent with studies applying other types of
573 non-invasive brain stimulation in healthy young adults, both in the context of motor learning (see
574 [107] for a meta-analysis), and reward tasks (e.g., [108,109]), despite the much longer stimulation time
575 used in these studies (between 3 and 20 times longer). Overall, albeit moderate, we believe that
576 the present effect sizes are relevant and consistent with what can be expected from the non-
577 invasive brain stimulation literature.

578

579 **Limitations**

580 The present study includes some limitations that we would like to acknowledge. First, at
581 the imaging level, we did not find a significant effect of reinforcement at the whole-brain level. This
582 might be due to the short duration of the task (6x40s), combined with the fact that we did not
583 couple reinforcement to monetary incentives, a manipulation known to strongly boost striatal
584 activity in the context of motor learning[18]. Yet, when considering BOLD activity in the striatal ROIs,
585 we did find a significant effect of reinforcement, suggesting that our experimental manipulation did
586 increase striatal activity but that the strength of the effect was insufficient to survive at the whole-

587 brain level. Second, we did not find any effect of tTIS when considering averaged BOLD activity.
588 Again, the short duration of the blocks may contribute to this non-significant effect. Another
589 possible interpretation is that the effect of tTIS on BOLD activity is not uniform across participants
590 as it likely depends on individual anatomy and function of the targeted brain region, as observed
591 for other non-invasive brain stimulation techniques[110]. Consistently, we found a correlation
592 between levels of impulsivity and the neural effects of $tTIS_{80Hz}$ (both BOLD and connectivity, Figure
593 S7). Importantly though, when including learning as a behavioral regressor we did find significant
594 clusters of correlation specifically in the striatum (Figure 3), suggesting that the behavioural effects
595 were indeed related to modulation of activity in the target region. Notably, this result was significant
596 when contrasting $tTIS_{80Hz}$ to the active control ($tTIS_{20Hz}$), but not to $tTIS_{Sham}$. Overall, we believe
597 that the fMRI data does provide interesting support that the behavioural effects of the stimulation
598 were indeed related to modulation of neural activity in the striatum, also in line with the present
599 simulations on realistic head models (Figure 1) and the connectivity results (Figure 4). This idea
600 is also in agreement with another recent study investigating the effects of tTIS on motor sequence
601 learning[52]. Notably though, a limitation of the present dataset is the very short duration of
602 stimulation and imaging for each experimental condition, that may explain some inconsistencies
603 in the results. Hence, following this first proof-of-concept study showing robust behavioural effects
604 and related neural changes, future studies including longer fMRI and stimulation sessions are
605 required to further confirm these results.

606 Finally, within the present study the computational modelling was performed on a realistic,
607 detailed head model (i.e., the MIDA model[59], see Methods). One limitation of this approach is that
608 the electric field simulations do not take individual structural information into account. Such
609 individual modeling would require information on brain anisotropy, an aspect that is likely to
610 significantly influence tTIS exposure[44,111]. However, in the present study diffusion MRI to evaluate

611 fractional anisotropy was not acquired. Future studies including diffusion MRI data will allow for
612 personalised modelling, paving the way for individualised tTIS informed by brain structure[53].

613

614 **Conclusion**

615 The present findings show for the first time the ability of non-invasive striatal tTIS to
616 interfere with reinforcement learning in humans through a selective modulation of striatal activity
617 and support the causal functional role of the human striatum in reinforcement motor learning. This
618 deep brain stimulation was well tolerated and compatible with efficient blinding, suggesting that
619 tTIS provides the exciting option to circumvent the steep depth-focality trade-off of current non-
620 invasive brain stimulation approaches in a safe and effective way. Overall, tTIS opens new
621 possibilities for the study of causal brain-behaviour relationships and for the treatment of neuro-
622 psychiatric disorders associated to alterations of deep brain structures.

623 # 4. Methods

624 ## 4.1. Participants

625

626 A total of 48 right-handed healthy volunteers participated in the study. 24 participants were
627 enrolled for the main tTIS study (15 women, 25.3 ± 0.7 years old; mean ± SE). Another group of
628 24 volunteers participated in the behavioural control experiment (Figure S2, 14 women, 24.2 ± 0.5
629 years old). Handedness was determined via a shortened version of the Edinburgh Handedness
630 inventory[112] (laterality index = 89.3 ± 2.14% for the main study and 86.4 ± 2.51% for the control
631 experiment). None of the participants suffered from any neurological or psychiatric disorder, nor
632 taking any centrally-acting medication (see Supplementary Materials for a complete list of
633 exclusion criteria). All participants gave their written informed consent in accordance with the
634 Declaration of Helsinki and the Cantonal Ethics Committee Vaud, Switzerland (project number
635 2020-00127). Finally, all participants were asked to fill out a delay-discounting monetary choice
636 questionnaire[113], which evaluates the propensity of subjects to choose smaller sooner rewards
637 over larger later rewards, a preference commonly associated to choice impulsivity[75,114].

638

639 ## 4.2. Experimental procedures

640

641 The study employed a randomised, double-blind, sham-controlled design. Following
642 screening and inclusion, participants were invited to a single experimental session including
643 performance of a motor learning task with concurrent transcranial electric Temporal Interference
644 stimulation (tTIS) of the striatum and functional magnetic resonance imaging (fMRI). Overall,
645 participants practiced 6 blocks of trials, that resulted from the combination of two reinforcement
646 feedback conditions ($Reinf_{TYPE}$: $Reinf_{ON}$ or $Reinf_{OFF}$) with three types of striatal stimulation
647 ($tTIS_{TYPE}$: $tTIS_{Sham}$, $tTIS_{20Hz}$ or $tTIS_{80Hz}$).

648

649 4.2.1. Motor learning task

650

651 4.2.1.1. General aspects

652

653 Participants practiced an adaptation of a widely used force-tracking motor task[54,55] with a
654 fMRI-compatible fiber optic grip force sensor (Current designs, Inc., Philadelphia, PA, USA)
655 positioned in their right hand. The task was developed on Matlab 2018 (the Mathworks, Natick,
656 Massachusetts, USA) exploiting the Psychophysics Toolbox extensions[115,116] and was displayed
657 on a computer screen with a refresh rate of 60 Hz. The task required participants to squeeze the
658 force sensor to control a cursor displayed on the screen. Increasing the exerted force resulted in
659 the cursor moving vertically and upward in a linear way. Each trial started with a preparatory period
660 in which a sidebar appeared at the bottom of the screen (**Figure 1A**). After a variable time interval
661 (0.9 to 1.1 s), a cursor (black circle) popped up in the sidebar and simultaneously a target (grey
662 larger circle with a cross in the middle) appeared, indicating the start of the movement period.
663 Subjects were asked to modulate the force applied on the transducer to keep the cursor as close
664 as possible to the center of the target. The target moved in a sequential way along a single vertical
665 axis for 7 s. The maximum force required (i.e., the force required to reach the target when it was
666 in the uppermost part of the screen; $MaxTarget_{Force}$) was set at 4% of maximum voluntary
667 contraction (MVC) evaluated at the beginning of the experiment. This low force level was chosen
668 based on pilot experiments to limit muscular fatigue. Finally, each trial ended with a blank screen
669 displayed for 2 s before the beginning of the next trial.

670

671 4.2.1.2. Trial types and reinforcement manipulation

672

673 During the experiment, participants were exposed to different types of trials (**Figure 1A,**
674 **Video S1**). In Test trials, the cursor remained on the screen and the target was consistently
675 displayed in grey for the whole duration of the trial. These trials served to evaluate Pre- and Post-
676 training performance for each block, without any disturbance. In $Reinf_{ON}$ and $Reinf_{OFF}$ trials (used
677 during Training only), we provided only partial visual feedback to the participants in order to
678 increase the impact of reinforcement on learning[4,56–58]. As such, the cursor was only intermittently
679 displayed during the trial: it was always displayed in the first second of the trial, and then
680 disappeared for a total of 4.5 s randomly split on the remaining time by bits of 0.5 s. The cursor
681 was therefore displayed 35.7% of the time during these trials (2.5 s over the 7 s trial). Importantly,
682 contrary to the cursor, the target always remained on the screen for the whole trial and participants
683 were instructed to continue to track the target even when the cursor was away.

684 In addition to this visual manipulation, in $Reinf_{ON}$ trials, participants also trained with
685 reinforcement feedback indicating success or failure of the tracking in real time. As such,
686 participants were informed that, during these trials, the color of the target would vary as a function
687 of their performance: the target was displayed in green when tracking was considered as
688 successful and in red when it was considered as failure. Online success on the task was
689 determined based on the Error, defined as the absolute force difference between the force
690 required to be in the center of the target and the exerted force[4,54–56]. The Error, expressed in
691 percentage of MVC, was computed for each frame refresh and allowed to classify a sample as
692 successful or not based on a closed-loop reinforcement schedule[8]. More specifically, for each
693 training trial, a force sample (recorded at 60 Hz, corresponding to the refresh rate of the monitor)
694 was considered as successful if the computed Error was below the median Error over the 4
695 previous trials at this specific sample. Put differently, to be successful, participants had to
696 constantly beat their previous performance. This closed-loop reinforcement schedule allowed us
697 to deliver consistent reinforcement feedback across individuals and conditions (see control

698 analysis on success rates in the Supplementary materials), while maximizing uncertainty on the
699 presence of reinforcement, an aspect that is crucial for efficient reinforcement motor learning[117].
700 Notably, in addition to this closed-loop design, samples were also considered as successful if the
701 cursor was very close to the center of the target (i.e., within one radius around the center,
702 corresponding to an Error below 0.2% of MVC). This was done to prevent any conflict between
703 visual information (provided by the position of the cursor relative to the target) and reinforcement
704 feedback (provided by the color of the target), which could occur in situations of extremely good
705 performance (when the closed-loop Error cut-off is below 0.2% of MVC).

706 As a control, $Reinf_{OFF}$ trials were similar to $Reinf_{ON}$ trials with the only difference that the
707 displayed colors were either cyan or magenta, and were generated randomly. Participants were
708 explicitly told that, in this condition, colors were displayed randomly and could be ignored. The
709 visual properties of the target in the $Reinf_{OFF}$ condition were designed to match the $Reinf_{ON}$
710 condition in terms of relative luminance (cyan: RGB = [127.5 242.1 255] matched to green: [127.5
711 255 127.5] and magenta: [211.7 127.5 255] to red: [255 127.5 127.5]) and average frequency of
712 change in colors (i.e., the average number of changes in colors divided by the total duration of a
713 trial, see Supplementary materials).

714 Notably, in this task, Training trials differed from Test trials regarding not only the color of
715 the target (red/green or cyan/magenta in Training trials and grey in Test trials) but also the visual
716 feedback experienced (partial and full visual feedback in Training and Test trials, respectively).
717 This choice was motivated by several reasons. First, we wanted to evaluate learning in the
718 classical, unperturbed, version of the force-tracking task[54,55], which is compatible with clinical
719 translation. Second, based on additional behavioural data on another group of participants (n =
720 24, see Figure S2), we found that significant effects of reinforcement on learning were observed
721 only when training was performed with partial visual feedback (displayed on 35.7% of the trial
722 time, as in the present study), in line with previous results[57,62]. However, this additional study also

723 revealed very limited improvement of performance during training with partial visual feedback,
724 potentially due to ceiling effects on performance in this condition. Yet, the improvement of
725 performance when comparing the Pre and Post-training assessments strongly suggested that
726 practicing the task with partial visual feedback still induced significant learning of the skill. Finally,
727 the change in visual feedback between Training and Post-training was the same in all
728 experimental conditions; this aspect of the task is therefore unlikely to explain the reinforcement
729 as well as the stimulation effects reported here.

730 Even though our study focused on reinforcement motor learning, it is worth mentioning that
731 other learning mechanisms such as error-based or strategic processes are likely to be also
732 engaged during the force-tracking task and may have recruited other brain regions beyond the
733 striatum (Spampinato and Celnik, 2020). Notably though, our protocol was specifically designed
734 to compare in the same individuals, learning in $Reinf_{ON}$ and $Reinf_{OFF}$ conditions while keeping the
735 other parameters of the task constant, to specifically isolate the contribution of reinforcement
736 processes in motor learning.

737

738 4.2.1.3. Motor learning protocol

739

740 After receiving standardised instructions about the force-tracking task, participants
741 practiced 5 blocks of familiarization (total of 75 trials) without tTIS. The first block of familiarization
742 included 20 trials with the target moving in a regular fashion (0.5 Hz sinuoid). Then, in a second
743 block of familiarization, participants performed 35 trials of practice with an irregular pattern, with
744 the same properties as the training patterns (see below). Finally, we introduced the reinforcement
745 manipulation and let participants perform 2 short blocks (8 trials each) including $Reinf_{ON}$ and
746 $Reinf_{OFF}$ trials. These four first blocks of familiarization were performed outside the MRI
747 environment. A last familiarization block (4 trials) was performed after installation in the scanner,

748 to allow participants to get used to performing the task in the MRI. This long familiarization allowed
749 participants to get acquainted with the use of the force sensor, before the beginning of the
750 experiment.

751 During the main part of the experiment, participants performed 6 blocks of trials in the MRI
752 with concurrent striatal tTIS (**Figure 1B**). Each block was composed of 4 Pre-training trials
753 followed by 24 Training and 8 Post-training trials. Pre- and Post-training trials were performed in
754 Test conditions, without tTIS and were used to evaluate motor learning. Training trials were
755 performed with or without reinforcement feedback and with concomitant striatal tTIS and were
756 used as a proxy of motor performance. During Training, trials were interspersed with 25 s resting
757 periods every 4 trials (used for fMRI contrasts, see below). The order of the 6 experimental
758 conditions was pseudo-randomised across participants: the 6 blocks were divided into 3 pairs of
759 blocks with the same tTIS condition and each pair was then composed of one $Reinf_{ON}$ and one
760 $Reinf_{OFF}$ block. Within this structure, the order of the $tTIS_{TYPE}$ and $Reinf_{TYPE}$ conditions were
761 balanced among the 24 participants. Hence, this randomisation allowed us to ensure that any
762 order effect that may arise from the repetition of the learning blocks would have the same impact
763 on each experimental condition (e.g., 4 subjects experienced $tTIS_{80Hz}$ - $Reinf_{ON}$ in the first block, 4
764 other subjects in the second block, 4 in the third block etc.).

765 As mentioned above, the protocol involved multiple evaluations of motor learning within
766 the same experimental session. In order to limit carry-over effects from one block to the following,
767 each experimental block was associated to a different pattern of movement of the target (**Figure**
768 **S1**). Put differently, in each block, participants had to generate a new pattern of force to
769 successfully track the target. To balance the patterns' difficulty, they all consisted in the summation
770 of 5 sinusoids of variable frequency (range: 0.1-1.5 Hz) that presented the following properties: a)
771 Average force comprised between 45 and 55% of the $MaxTarget_{Force}$; b) Absolute average
772 derivative comprised between 54 and 66 % of the $MaxTarget_{Force}$/s; c) Number of peaks = 14

773 (defined as an absolute change of force of at least 1% of $MaxTarget_{Force}$). These parameters were
774 determined based on pilot experiments to obtain a relevant level of difficulty for young healthy
775 adults and consistent learning across the different patterns.

776

777 4.2.2. Transcranial Electric Temporal Interference Stimulation (tTIS) applied to the
778 striatum

779

780 4.2.2.1. General concept

781

782 Transcranial temporal interference stimulation (tTIS) is an innovative non-invasive brain
783 stimulation approach, in which two or more independent stimulation channels deliver high-
784 frequency currents in the kHz range (oscillating at f1 and f1 + Δf; **Figure 1C**). These high-
785 frequency currents are assumed to be too high to effectively modulate neuronal activity [41,50,118].
786 Still, by applying a small shift in frequency, they result in a modulated electric field with the
787 envelope oscillating at the low-frequency Δf (target frequency) where the two currents overlap.
788 The peak of the modulated envelope amplitude can be steered towards specific areas located
789 deep in the brain, by tuning the position of the electrodes and current ratio across stimulation
790 channels[41] (**Figure 1C, 1D**). Based on these properties, tTIS has been shown to be able to focally
791 target activity of deep structures in rodents, without engaging overlying tissues[41]. Here, we applied
792 temporal interference stimulation transcranially via surface electrodes applying a low-intensity,
793 sub-threshold protocol following the currently accepted cut-offs and safety guidelines for low-
794 intensity transcranial electric stimulation in humans[119].

795

796 4.2.2.2. Stimulators

797

The currents for tTIS were delivered by two independent DS5 isolated bipolar constant current stimulators *(Digitimer Ltd, Welwyn Garden City, UK)*. The stimulation patterns were generated using a custom-based Matlab graphical user interface and transmitted to the current sources using a standard digital-analog converter *(DAQ USB-6216, National Instruments, Austin, TX, USA)*. Finally, an audio transformer was added between stimulators and subjects, in order to avoid possible direct current accumulation.

4.2.2.3. Stimulation protocols

During the 6 Training blocks, we applied three different types of striatal tTIS (2 blocks each): a stimulation with a tTIS envelope modulated at 20Hz ($tTIS_{20Hz}$), a stimulation with a tTIS envelope modulated at 80Hz ($tTIS_{80Hz}$) and a sham stimulation ($tTIS_{Sham}$). For $tTIS_{20Hz}$, the posterior stimulation channel (TP7-TP8, see below) delivered a 1.99 kHz stimulation while the anterior one delivered a 2.01 kHz (Δf = 20 Hz). For $tTIS_{80Hz}$, the posterior and anterior channels delivered 1.96 kHz and 2.04 kHz, respectively (Δf = 80 Hz). Hence in both conditions, the high frequency component was comparable and the only difference was Δf. During each block, tTIS was applied for 5 minutes (6 x 50 s) during Training. Each stimulation period started and ended with currents ramping-up and -down, respectively, for 5 s. tTIS was applied only while participants were performing the motor task and not during resting periods or Pre- and Post-training assessments. Finally, $tTIS_{Sham}$ consisted in a ramping-up (5 s) immediately followed by a ramping-down (5 s) of 2 kHz currents delivered without any shift in frequency. This condition allowed us to mimic the sensations experienced during the active conditions $tTIS_{20Hz}$ and $tTIS_{80Hz}$, while delivering minimal brain stimulation (Figure S5). A trigger was sent 5 seconds before the beginning of each trial in order to align the beginning of the task and the beginning of the frequency shift after the ramp-up. Other tTIS parameters were set as follows: current intensity per stimulation

823 channel = 2 mA (baseline-to-peak), electrode type: round, conductive rubber with conductive
824 cream/paste, electrode size = 3 cm^2 (see ContES checklist in Supplementary materials for more
825 details).

826 The stimulation was applied within the MRI environment (Siemens 3T MAGNETOM
827 Prisma; Siemens Healthcare, Erlangen, Germany) using a standard RF filter module and MRI-
828 compatible cables *(neuroConn GmbH, Ilmenau, Germany)*. The technological, safety and noise
829 tests, and methodological factors can be found in Supplementary materials (Table S1) and are
830 based on the ContES Checklist [120].

831

832 4.2.2.4. Modelling

833

834 Electromagnetic simulations were carried out to identify optimised electrode placement
835 and current steering parameters. Simulations were performed using the MIDA head model[59], a
836 detailed anatomical head model featuring >100 distinguished tissues and regions that was derived
837 from multi-modal image data of a healthy female volunteer. Importantly, for brain stimulation
838 modelling, the model differentiates different scalp layers, skull layers, grey and white matter,
839 cerebrospinal fluid, and the dura and accounts for electrical conductivity anisotropy and neural
840 orientation based on diffusion tensor imaging (DTI) data. Circular electrodes (radius = 0.7 cm)
841 were positioned on the skin according to the 10-10 system and the electromagnetic exposure was
842 computed using the ohmic-current-dominated electro-quasistatic solver from Sim4Life v5.0 (ZMT
843 Zurich MedTech AG, Switzerland), which is suitable due to the dominance of ohmic currents over
844 displacement currents and the long wavelength compared with the simulation domain[121]. Dielectric
845 properties were assigned based on the IT'IS Tissue Properties Database v4.0[122]. Rectilinear
846 discretization was performed, and grid convergence as well as solver convergence analyses were
847 used to ensure negligible numerical uncertainty, resulting in a grid that included more than 54M

848 voxels. Dirichlet voltage boundary conditions, and then current normalization were applied. The
849 electrode-head interface contact was treated as ideal. tTIS exposure was quantified according to
850 the maximum modulation envelope magnitude formula from Grossman et al., (2017)[41]. Then, a
851 sweep over 960 permutations of the four electrode positions was performed, considering
852 symmetric and asymmetric montages with parallel (sagittal and coronal) or crossing current paths,
853 while quantifying bilateral striatum (putamen [BNA regions 225, 226, 229, 230], caudate [BNA
854 regions 219, 220, 227, 228] and nucleus accumbens [BNA regions 223, 224]) exposure
855 performance according to three metrics: a) target exposure strength, b) focality ratio (the ratio of
856 target tissue volume above threshold compared to the whole-brain tissue volume above threshold,
857 a measure of stimulation selectivity), and c) activation ratio (percentage of target volume above
858 threshold with respect to the total target volume, a measure of target coverage). We defined the
859 threshold as the 98th volumetric iso-percentile level of the tTIS. From the resulting Pareto-optimal
860 front, two configurations stood out particularly: one that maximised focality and activation (AF3 -
861 AF4, P7 - P8) and a second one that accepts a reduction of these two metrics by a quarter, while
862 increasing the target exposure strength by more than 50% (F3-F4, TP7-TP8). This last montage
863 was selected, to ensure sufficient tTIS exposure in the striatum[52] (Figure 1C, 1D).

864

865 4.2.2.5. Electrode positioning and evaluation of stimulation-associated sensations

866

867 Based on the modelling approach described above, we defined the stimulation electrode
868 positions in the framework of the EEG 10-10 system[123]. The optimal montage leading in terms of
869 target (i.e. the bilateral striatum) exposure strength and selectivity, was composed of the following
870 electrodes: F3, F4, TP7 and TP8. Their locations were marked with a pen on the scalp and, after
871 skin preparation (cleaned with alcohol), round conductive rubber electrodes of 3 cm^2 were placed
872 adding a conductive paste (*Ten20, Weaver and Company, Aurora, CO, USA or Abralyt HiCl,*
873 *Easycap GmbH, Woerthsee-Etterschlag, Germany*) as an interface to the skin. Electrodes were

874 held in position with tape and cables were oriented towards the top in order to allow good
875 positioning inside the scanner. Impedances were checked and optimised until they were below 20
876 kΩ [48]. Once good contact was obtained, we tested different intensities of stimulation for each
877 stimulation protocol in order to familiarise the participants with the perceived sensations and to
878 systematically document them. $tTIS_{Sham}$, $tTIS_{20Hz}$ and $tTIS_{80Hz}$ were applied for 20 seconds with the
879 following increasing current amplitudes per channel: 0.5 mA, 1 mA, 1.5 mA and 2 mA. Participants
880 were asked to report any kind of sensation and, if a sensation was felt, they were asked to grade
881 the intensity from 1 to 3 (light to strong) as well as give at least one adjective to describe it (Figure
882 S5). Following this step, cables were removed to be replaced by MRI-compatible cables and a
883 bandage was added to apply pressure on the electrodes and keep them in place. An impedance
884 check was repeated in the MRI right before the training and then again at the end of all recordings.

885

886 4.2.3. MRI data acquisition

887

888 Structural and functional images were acquired using a 3T MAGNETOM PRISMA scanner
889 (*Siemens, Erlangen, Germany*). T1-weighted images were acquired via the 3D MPRAGE
890 sequence with the following parameters: TR = 2.3 s; TE = 2.96 ms; flip angle = 9°; slices = 192;
891 voxel size = 1 × 1 × 1 mm, FOV = 256 mm. Anatomical T2 images were also acquired with the
892 following parameters: TR = 3 s; TE = 409 ms; flip angle = 120°; slices = 208; voxel size = 0.8 ×
893 0.8 × 0.8 mm, FOV = 320 mm. Finally, functional images were recorded using Echo-Planar
894 Imaging (EPI) sequences with the following parameters: TR = 1.25 s; TE = 32 ms; flip angle =
895 58°; slices = 75; voxel size = 2 × 2 × 2 mm; FOV = 112 mm.

896

897 **4.3. Data and statistical analyses**

898

Data and statistical analyses were carried out with Matlab 2018a (the Mathworks, Natick, Massachusetts, USA) and the R software environment for statistical computing and graphics (R Core Team 2021, Vienna, Austria). Robust linear regressions were fitted with the Matlab function robustfit. Linear mixed models (LMM) were fitted using the lmer function of the lme4 package in R [124]. As random effects, we added intercepts for participants and block. Normality of residuals, and homoscedasticity of the data were systematically checked, and logarithmic transformations were applied when necessary (i.e., when skewness of the residuals' distribution was not comprised between - 2 and 2[125] or when homoscedasticity was violated based on visual inspection). To mitigate the impact of isolated influential data points on the outcome of the final model, we used tools of the influence.ME package to detect and remove influential cases based on the following criterion: distance > 4 * mean distance[126]. Statistical significance was determined using the anova function with Satterthwaite's approximations of the lmerTest package[127]. For specific post-hoc comparisons we conducted pairwise comparisons by computing estimated marginal means with the emmeans package with Tukey adjustment of p-values[128]. Standardised effect size measures were obtained using the eff_size function of the emmeans package[129]. The level of significance was set at $p<0.05$.

4.3.1. Behavioural data

4.3.1.1. Evaluation of motor learning

The main goal of the present study was to evaluate the influence of striatal tTIS on reinforcement motor learning. To do so, we first removed trials, in which participants did not react within 1 s after the appearance of the cursor and target, considering that these extremely long preparation times may reflect significant fluctuations in attention[130]. This occurred extremely rarely (0.52 % of the whole data set). For each subject and each trial, we then quantified the tracking

Error as the absolute force difference between the applied and required force as done previously[4,54,56]. Tracking performance during Training and Post-training trials were then normalised according to subjects' initial level by expressing the Error data in percentage of the average Pre-training Error for each block. In order to test our main hypothesis predicting specific effects of striatal tTIS on reinforcement motor learning, we performed a LMM on the Post-training data with $tTIS_{TYPE}$ and $Reinf_{TYPE}$ as fixed effects. We then also ran the same analysis on the Training data, to evaluate if striatal tTIS also impacted on motor performance, while stimulation was being delivered.

As a control, we checked that initial performance at Pre-training was not different between conditions with a LMM on the Error data obtained at Pre-training. Again, $tTIS_{TYPE}$ and $Reinf_{TYPE}$ were considered as fixed effects. Finally, another LMM was fitted with the fixed effect $tTIS_{TYPE}$ to verify that the amount of positive reinforcement (as indicated by a green target) in the $Reinf_{ON}$ blocks was similar across $tTIS_{TYPES}$.

4.3.2. fMRI data

4.3.2.1. Imaging Preprocessing

We analyzed functional imaging data using Statistical Parametric Mapping 12 (*SPM12; The Wellcome Department of Cognitive Neurology, London, UK*) implemented in MATLAB R2018a (*Mathworks, Sherborn, MA*). All functional images underwent a common preprocessing including the following steps: slice time correction, spatial realignment to the first image, normalization to the standard MNI space and smoothing with a 6 mm full-width half-maximal Gaussian kernel. T1 anatomical images were then co-registered to the mean functional image and segmented. This allowed to obtain bias-corrected gray and white matter images, by normalizing the functional images via the forward deformation field. To select subjects with acceptable level of head movement, framewise displacement was calculated for each run. A visual check of both non-

normalised and normalised images was performed in order to ensure good preprocessing quality. Finally, possible tTIS-related artifacts were investigated based on signal to noise ratio maps (see below).

4.3.2.2. Signal to Noise Ratio

Total signal to noise ratio (tSNR) maps were computed to check the presence of possible artifacts induced by the electrical stimulation. The values were calculated per each voxel by dividing the mean of the voxel time series by its standard deviation. Spherical regions of interest were then defined both underneath the tTIS electrodes and at 4 different locations, distant from the electrodes as a control. The center of each spherical ROI was obtained by projecting the standard MNI coordinates of each electrode on the scalp[131] toward the center of the brain. After visual inspection of the ROIs, average tSNR maps were extracted within each sphere. A LMM was used to compare the average SNR underneath the electrodes versus the control regions and between stimulation protocols. The results of this analysis are presented in Supplementary materials (Figure S8).

4.3.2.3. Task-based BOLD activity analysis

A general linear model was implemented at the single-subject level in order to estimate signal amplitude. Eight regressors were included in the model: 6 head motion parameters (displacement and rotation) and normalised time series within the white matter and the corticospinal fluid. Linear contrasts were then computed to estimate specific activity during the motor task with respect to resting periods. Functional activation was also extracted within specific ROIs individually defined based on structural images. More specifically, the Freesurfer recon-all function was run based on the structural T1w and T2w images

979 (https://surfer.nmr.mgh.harvard.edu/). The BNA parcellation was derived on the individual subject
980 space and the selected ROIs were then co-registered to the functional images and normalised to
981 the MNI space. BOLD activity within the individual striatal masks was averaged and compared
982 between different striatal nuclei namely the putamen (BNA regions 225, 226, 229, 230), caudate
983 (BNA regions 219, 220, 227, 228) and nucleus accumbens (BNA regions 223, 224). Comparison
984 between conditions were presented for uncorrected voxel-wise FWE, p=0.001 and multiple
985 comparison corrected at the cluster level to reduce False Discovery Rate (FDR), p=0.05.

986

987

988 4.3.2.4. Effective connectivity analyses

989

990 As an additional investigation, we computed task-modulated effective functional
991 connectivity by means of the CONN toolbox 2021a (www.nitrc.org/projects/conn,
992 RRID:SCR_009550) running in Matlab R2018a (*Mathworks, Sherborn, MA*). An additional
993 denoising step was added by applying a band-pass filtering from 0.01 to 0.1 Hz and by regressing
994 potential confounders (white matter, CSF and realignment parameters). After that, generalized
995 Psycho-Physiological Interactions (gPPI) connectivity was extracted within specific pre-defined
996 customised sub-networks: a reward and a motor network. gPPI evaluates condition-specific
997 changes in effective connectivity, defined as the directed effect that one brain region has on
998 another under some model of neuronal coupling (Friston, 1994). In particular, gPPI considers a
999 series of equations in which activity in a ROI (pre-defined frontal areas in our case) depends on a
1000 specific condition (the 'psychological' factor) and on activity in the seed region (striatum here, the
1001 'physiological' factor). By solving these equations, it is possible to determine a coefficient that
1002 represents task-modulation of effective connectivity[132]. Importantly, task-related changes in

1003 effective connectivity are expressed relative to rest, and therefore values closer to 0 reflect a
1004 connectivity similar to resting state.

1005

1006 The reward network was defined as following: two regions within the striatum, namely the
1007 NAc (BNA regions 223 and 224) and the ventro-medial putamen (BNA regions 225 and 226, left
1008 and right respectively), and two frontal areas, namely the anterior cingulate (BNA regions 177,
1009 179, 183 and 178, 180, 184, left and right respectively) and the orbitofrontal cortex within the
1010 vmPFC (BNA regions 41, 45, 47, 49, 187 and 42, 46, 48, 50, 188 for left and right respectively).
1011 The motor network included the following areas: the dorso-lateral putamen (BNA 229, 230, for left
1012 and right respectively), the dorsal caudate (BNA regions 227, 228 for left and right respectively)
1013 the medial part of the SMA (BNA regions 9 and 10, left and right respectively) and the part of the
1014 M1 associated to upper limb function (BNA regions 57 and 58, left and right respectively). Notably,
1015 we considered connectivity in the left and right motor and reward networks regardless of laterality.
1016 These ROIs were selected based on the following rationale. First, they are consistent with previous
1017 literature on reinforcement learning of motor skills[68,90,133,134]. Second, there is structural and
1018 functional evidence for these fronto-striatal connections[135,136]. Third, the frontal areas included in
1019 the analyses are well-established hubs of the motor learning (M1 and SMA, see [12] for a meta-
1020 analysis) and reward networks (vmPFC and ACC, see [11] for a meta-analysis). Finally, gPPI was
1021 also extracted within a control language network, defined based on the functional atlas described
1022 by Shirer et al.(2012)[70].

Supplementary material

1. Exclusion criteria

- Unable to consent
- Severe neuropsychiatric (e.g., major depression, severe dementia) or unstable systemic diseases (e.g., severe progressive and unstable cancer, life threatening infectious diseases)
- Severe sensory or cognitive impairment or musculoskeletal dysfunctions prohibiting to understand instructions or to perform the experimental tasks
- Color blindness
- Inability to follow or non-compliance with the procedures of the study
- Contraindications for NIBS or MRI:
    - Electronic or ferromagnetic medical implants/device, non-MRI compatible metal implant
    - History of seizures
    - Medication that significantly interacts with NIBS being benzodiazepines, tricyclic antidepressant and antipsychotics
- Regular use of narcotic drugs
- Left-handedness
- Pregnancy
- Request of not being informed in case of incidental findings
- Concomitant participation in another trial involving probing of neuronal plasticity.

2. ContES Checklist

Technological factors	
Manufacturer of Stimulator	DS5 Isolated Bipolar Constant Current Stimulator (Digitimer)
MR Conditional Electrode Details	Round, 3 cm2 conductive rubber electrodes
Electrode Positioning	F3 → F4 TP7 → TP8 A bandage is warped around the head to apply pressure and keep the electrodes in place Electrodes are oriented in order to have vertical cables entering parallel to the MRI coil Head was fixed with pillows to avoid movements
MR Conditional Skin-Electrode Interface	10-20 gel One or two drops of saline were added when impedances were too high
Amount of Contact Medium (Paste/Gel/Electrolyte)	Around 1mm of paste was manually placed on the electrodes
Electrode Placement Visualization	Pictures 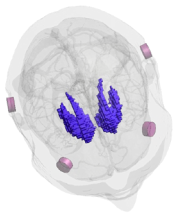

RF Filter	NeuroConn DC-STIMULATOR MR RF filter module with MRI-compatible cables and electrodes
Wire Routing Pattern	10 m ethernet cables between inner and outer box pass through a conduit along the wall of the MRI room until reaching the back of the MRI. Cables are then fixed with straps on the ground and on the wall of the MRI machine in order to avoid loops until reaching the interior of the coil. Cables between the head and the inner boxes were also fixed with straps and they were oriented in order to exit the magnetic field direction as soon as possible as indicated by the red arrows of the image below.
tES-fMRI Machine Synchronization/Communication	Stimulation was triggered by the stimulus delivery PC via parallel port to BNC cable. The parallel port of the stimulus delivery PC was connected to the DAQ controlling the stimulators. Stimulus delivery PC, in turn, was also receiving the scanner trigger from the scanner via USB port.
Safety and noise tests	
MR Conditionality Specifics for tES Setting	Please refer to Section “Methods-Imaging acquisition”
tES-fMRI Setting Test - Safety Testing	Impedances were checked before and after

	the stimulation. No temperature tests were performed during the experiment. Intensity titration was performed prior to entering the MRI, testing increasing currents (0.5, 1, 1.5 and 2 mA) and asking the subject to report any type of sensation. A sensation questionnaire was also performed at the end of the experiment.
tES-fMRI Setting Test - Subjective Intolerance Reporting	No intolerances were reported by any subject
tES-fMRI Setting Test - Noise/Artifact	Signal to Noise Ratio (SNR) analysis was performed on the fMRI images, please refer to Section “Methods-Signal to Noise Ratio”
Impedance Testing	Impedances were checked right after electrodes positioning outside the scanner, before and after the stimulation inside. One or two drops of saline solution were added if impedances were higher than 20kΩ
Methodological factors	
Concurrent tES-fMRI Timing	For timings, please refer to the “Methods-Stimulation protocols” section To mitigate the impact of potential carry-over effects on our experimental results we used the following strategy: 1) We stimulated for short periods in each condition (5 minutes interspersed with resting periods without stimulation; see “Methods-Stimulation protocols”); 2) We imposed breaks (~7-8 minutes) between each stimulation protocol; 3) We randomised the order of the

	Stimulation conditions
Imaging Session Timing	All sequences were performed with TI stimulation electrodes placed on the subjects' head.
tES Experience Report	Please refer to "Results" section and to Figure S5.

Table S1. ContES checklist as recommended in Ekhtiari et al., 2022[120] for concurrent tES-fMRI studies.

3. Patterns of motion of the target used in the study

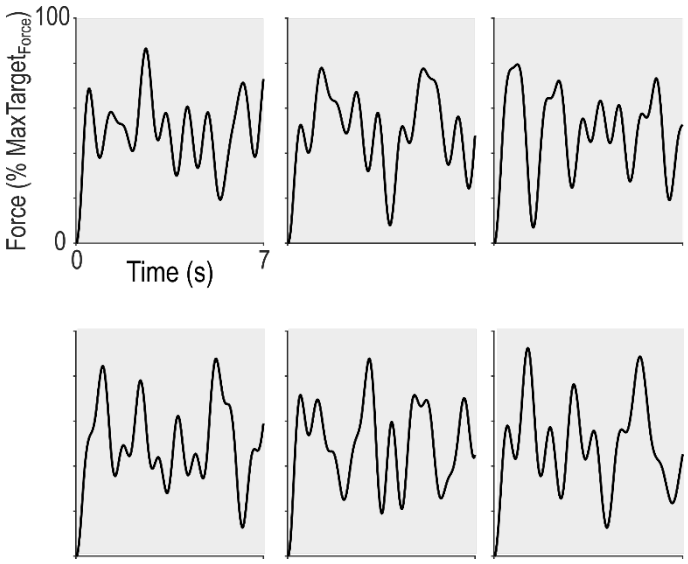

Figure S1. Patterns of motion of the target. For each block of training, participants had to learn a new pattern of motion of the target. The patterns had similar mathematical properties and their relationship to a condition was randomised (see Methods for more details).

4. Additional behavioural experiment

To determine the optimal experimental parameters to study reinforcement learning of motor skills, we performed an additional behavioural experiment, in the absence of brain stimulation and imaging. In particular, we tested the relationship between the amount of visual feedback available during Training and the benefits of reinforcement in the force-tracking task. Another group of young healthy participants (n=24; 14 women, 24.2 ± 0.5 years old, independent

1065 from the subjects tested in the main experiment) performed blocks of the task with $Reinf_{ON}$ or
1066 $Reinf_{OFF}$ and with either full visual feedback or only partial visual feedback (cursor displayed for
1067 35.7% of the total trial duration, as in the main study). Each learning block was composed of 30
1068 trials (vs. 36 trials in the main study) and in addition to real-time closed-loop reinforcement
1069 feedback, participants also received endpoint feedback on their overall performance after each
1070 trial during Training (i.e., indicating success or failure on the trial). The LMM ran on the Post-
1071 training data revealed a significant effect of visual feedback ($F_{(1,788.33)}$=5.90; p=0.015),
1072 reinforcement ($F_{(1,787.87)}$=11.64; p<0.001) and a significant interaction between these two factors
1073 ($F_{(1,788.03)}$=10.27; p=0.0014, **Figure S2A**). Interestingly, Tukey-corrected post-hoc tests showed
1074 that the interaction was due to the fact that while reinforcement did not improve learning when
1075 Training was performed with full visual feedback (p=0.88, d=0.014), it induced robust benefits
1076 when training with partial visual feedback (p<0.001, d=0.46, **Figure S2B**). This result is in line with
1077 previous literature showing that reinforcement feedback is particularly beneficial for motor learning
1078 when visual feedback is uncertain[57,62]. Based on the outcome of this additional study, we decided
1079 to train participants with partial visual feedback in the present experiment to evaluate the effect of
1080 tTIS in a version of the task that yielded significant reinforcement gains. Notably, this work also
1081 shows that the effect of reinforcement on motor learning observed in the $tTIS_{Sham}$ and $tTIS_{20Hz}$
1082 conditions (Figure 2) is reproducible.

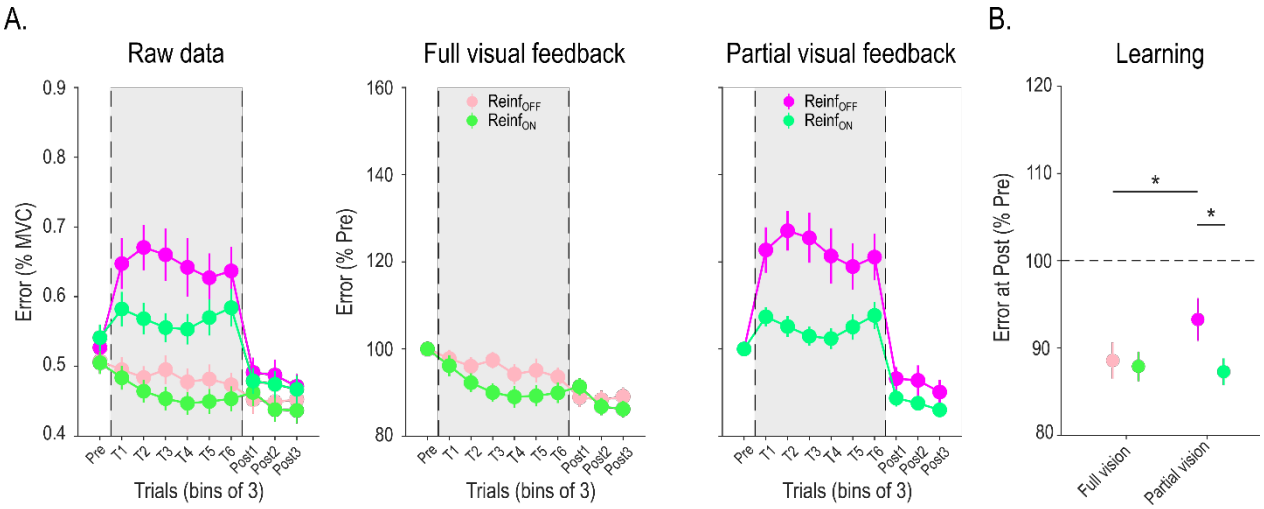

Figure S2. Results of an additional behavioural experiment (n = 24). A) Motor performance across training. Raw Error data (expressed in % of Maximum Voluntary Contraction [MVC]) are presented on the left panel for the different experimental conditions in bins of 3 trials. On the right, the two plots represent the Pre-training normalised Error in the Full visual feedback and Partial visual feedback blocks (i.e., cursor displayed 35.7% of the time, as in the main experiment). Note the strong gains in motor performance, especially with partial visual feedback but also the limited improvement of performance during training in this condition. **B) Motor learning.** Averaged Error at Post-training (normalised to Pre-training) in the different experimental conditions are shown, for the subjects included in the analysis (i.e., after outlier detection, n=23). Reduction of Error at Post-training reflects true improvement at tracking the target in Test conditions (in the absence of reinforcement or visual uncertainty). The LMM ran on these data revealed significant a significant effect of reinforcement feedback on learning when training with partial, but not full, visual feedback. *: p<0.05. Data are represented as mean ± SE.

5. Evolution of motor performance in the different conditions

The main analysis revealed a general effect of tTIS on motor performance during Training, irrespective of the presence of reinforcement. As a subsequent analysis, we also asked whether the evolution of performance during Training depended on type of striatal stimulation applied. We ran the same LMM as in the main study (see Results) but with the addition of a continuous fixed effect Trial, allowing us to evaluate whether the slope of performance change was different according to $tTIS_{TYPE}$. (**Figure S3**). Indeed, this analysis revealed a significant $tTIS_{TYPE}$ x Trial interaction ($F_{(2, 3399)}$=4.46; p=0.012) that was due to different slopes in the $tTIS_{Sham}$ compared to the $tTIS_{20Hz}$ (p=0.013) and $tTIS_{80Hz}$ (at the trend level, p=0.068) conditions. Evolution of performance in the $tTIS_{20Hz}$ and $tTIS_{80Hz}$ conditions was not different (p=0.81). Notably, this effect

could not be explained by differences in initial performance (all $p>0.21$ when comparing intercepts). Moreover, the effect of tTIS on motor improvement during Training did also not depend on the presence of reinforcement ($Reinf_{TYPE}$, $tTIS_{TYPE}$ and Trial: $F_{(2, 3399)}=0.51$; $p=0.60$). Overall, this analysis shows that the detrimental effect of striatal tTIS on motor performance is due to an impaired ability to improve performance with practice and further confirms that tTIS did not modulate the ability to use reinforcement feedback during Training.

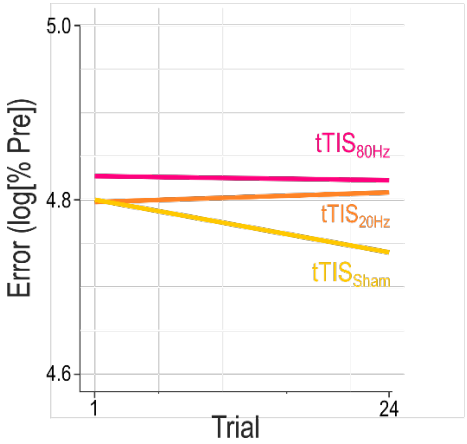

Figure S3. Slopes of performance change during Training in the different stimulation conditions. Modeled performance change for $tTIS_{Sham}$, $tTIS_{20Hz}$ and $tTIS_{80Hz}$ throughout Training. The $tTIS_{TYPE}$ x Trial interaction revealed that performance improved more with $tTIS_{Sham}$ compared to $tTIS_{20Hz}$ and $tTIS_{80Hz}$. Notably this effect was not modulated by the presence of reinforcement and could not be explained by differences in intercepts.

6. Effect of visual and reinforcement feedback on motor performance

As a control, we asked whether the tTIS and reinforcement effects reported in Figure 2 depended on the availability of visual information during Training. To do so, we computed the normalised Error for phases with the $Cursor_{ON}$ or $Cursor_{OFF}$ (taking into account a lag of 0.25s, corresponding to the estimated visuo-motor delay in this type of task for young healthy subjects[137]) and analysed these data in a LMM including the factors $Reinf_{TYPE}$, $tTIS_{TYPE}$ and $Cursor_{TYPE}$. As in the main analysis, we confirmed the effect of $Reinf_{TYPE}$ ($F_{(1, 6872)}=344.87$; $p<0.001$), $tTIS_{TYPE}$ ($F_{(2,6872)}=28.79$; $p<0.001$) and the absence of interaction between these two factors ($F_{(2,6875.4)}=0.49$;

p=0.61, Figure S4). This analysis also revealed a $Cursor_{TYPE}$ effect ($F_{(2,6875.3)}$=49.66; p<0.001) which was due to the fact that the Error was generally higher in the absence visual information on the position of the cursor (d=0.17). Interestingly, there was also a $Reinf_{TYPE}$ x $Cursor_{TYPE}$ interaction ($F_{(2,6872)}$=29.35; p<0.001): while benefits of reinforcement were significant in both the $Cursor_{ON}$ (p<0.001, d=0.32) and $Cursor_{OFF}$ (p<0.001, d=0.58) conditions, the magnitude of the reinforcement-related gains in performance were larger in the $Cursor_{OFF}$ condition (t-test comparing the gains: $t_{(46)}$=2.74, p=0.0086). Moreover, post-hoc tests also revealed that the absence of vision of the cursor was detrimental for performance in the $Reinf_{OFF}$ condition (p<0.001, d=0.30) but not in presence of $Reinf_{ON}$ (p=0.25, d=0.039). Hence, the presence of reinforcement was particularly beneficial when visual information was not available, in line with previous research[57,62] and also in agreement with the results of our additional experiment (Figure S2). Importantly, the LMM did not reveal any interaction between $tTIS_{TYPE}$ and $Cursor_{TYPE}$ ($F_{(2,6872)}$=0.49; p=0.31) and no triple interaction ($F_{(2,6872)}$=1.53; p=0.22), confirming that striatal tTIS had a global effect on motor performance during Training, which did not depend on the presence of visual and reinforcement feedback.

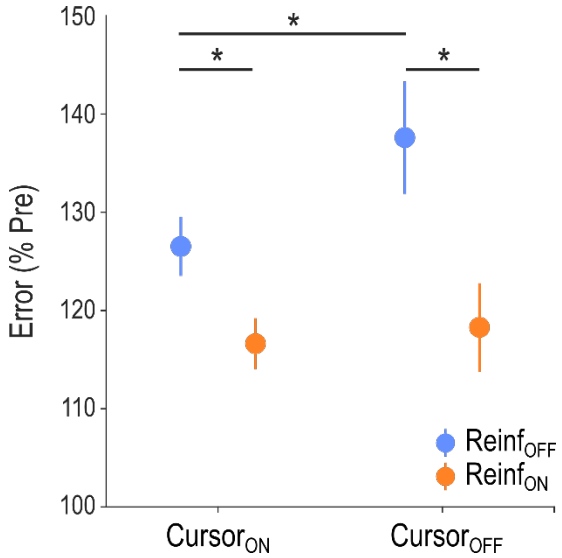

Figure S4. Effect of visual and reinforcement feedback on motor performance. Pre-training normalised Error depending on the presence of the cursor ($Cursor_{ON}$ or $Cursor_{OFF}$), and

the presence of reinforcement feedback during Training. The significant $Reinf_{TYPE}$ x $Cursor_{TYPE}$ interaction was related to the fact that the benefits of reinforcement were stronger when visual information was not available. Notably, this analysis takes into account a visuo-motor delay of 0.25s, as previously reported during a similar task (Lam and Zenon, 2021). *: $p<0.05$. Data are represented as mean ± SE.

7. Control analyses of behavioural data

Pre-training performance

In order to verify that our main behavioural results were not influenced by potential differences in initial performance between conditions despite randomisation, we analysed the Error at Pre-training between conditions. We did not find any $tTIS_{TYPE}$ ($F_{(2,519.15)}=1.64$; $p=0.20$) or $tTIS_{TYPE}$ x $Reinf_{TYPE}$ effect ($F_{(2,519.99)}=1.08$; $p=0.34$), suggesting that the main behavioural results could not be accounted for by differences in initial performance between conditions. However, the LMM did reveal a $Reinf_{TYPE}$ effect ($F_{(1,519.15)}=12.47$; $p<0.001$), that was due to the fact that Pre-training performance was generally better in $Reinf_{OFF}$ blocks. This effect, which was opposite to our learning results (generally better learning with $Reinf_{ON}$), may be related to an expectancy effect stemming from the repetitive structure of the reinforcement conditions (see Methods). However, the absence of interaction with $tTIS_{TYPE}$ is strongly suggestive that this effect did not drive any of the main findings. Put together, these data provide confidence that the differential effects of striatal tTIS on motor learning depending on the presence of reinforcement were not the result of different initial performance between conditions.

Success rate

Overall, the amount of positive reinforcement (i.e., when the target was green) averaged 52.78 +/- 0.42% and was comparable across $tTIS_{TYPES}$ ($F_{(2,1702)}=0.17$; $p=0.84$), suggesting that the closed-loop reinforcement schedule was successful at providing similar reinforcement feedback

1178 despite differences in performance between conditions. Hence, different success rates during
1179 training cannot explain the effect of the different striatal tTIS conditions on motor learning.

1180 Frequency of flashing

1181 Analysis of the frequency of flashing in the different conditions did not reveal any effect of
1182 $tTIS_{TYPE}$ ($F_{(2,3283)}$=0.85; p=0.43) nor any $Reinf_{TYPE}$ x $tTIS_{TYPE}$ interaction ($F_{(2,3283)}$=0.19; p=0.82),
1183 suggesting that the behavioural effects of tTIS could not be explained by a visual confound.
1184 However, this analysis did reveal a $Reinf_{TYPE}$ effect ($F_{(1,3283)}$=33.62; p<0.001) which was due to the
1185 fact that the average frequency in the $Reinf_{OFF}$ condition (4.28 ± 0.097 Hz) was slightly but
1186 significantly higher than with $Reinf_{ON}$ (4.08 ± 0.098 Hz; $F_{(1,3283)}$=33.62; p<0.001). Notably, in
1187 absolute terms, this difference represented only a difference of 1.4 change of color over the whole
1188 7 s trial, which we think is unlikely to explain the improvement of performance in the $Reinf_{ON}$
1189 condition.

1190 Order of the reinforcement conditions

1191 Previous exposure to reinforcement feedback may improve subsequent learning through
1192 reinforcement[138]. Thanks to our randomisation procedure, the previous exposure to the $Reinf_{ON}$
1193 condition was equally counterbalanced in all stimulation conditions, and should therefore not
1194 influence our main results. Still, we performed an analysis to specifically investigate the effect of
1195 the previous exposure to $Reinf_{ON}$. To do so, we split the participants depending on whether they
1196 experienced $Reinf_{ON}$ or $Reinf_{OFF}$ first (12 subjects per group) and performed a new LMM on the
1197 Post-training data with the addition of a categorical factor $Group_{TYPE}$. In particular, if the previous
1198 exposure to the $Reinf_{ON}$ condition influenced following learning with reinforcement, we would
1199 expect to see a $Group_{TYPE}$ x $Reinf_{TYPE}$ interaction. The analysis did not indicate any $Group_{TYPE}$
1200 effect on learning ($F_{(1,21.96)}$=0.35; p=0.56), neither did it reveal a $Group_{TYPE}$ x $Reinf_{TYPE}$ ($F_{(1,4)}$=0.72;
1201 p=0.44), or a triple interaction with $tTIS_{TYPE}$ ($F_{(2,1105.06)}$=1.75; p=0.17). Overall, this analysis

suggests that the order of the exposure to the reinforcement condition did not influence the present findings.

8. Blinding integrity and tTIS-evoked sensations

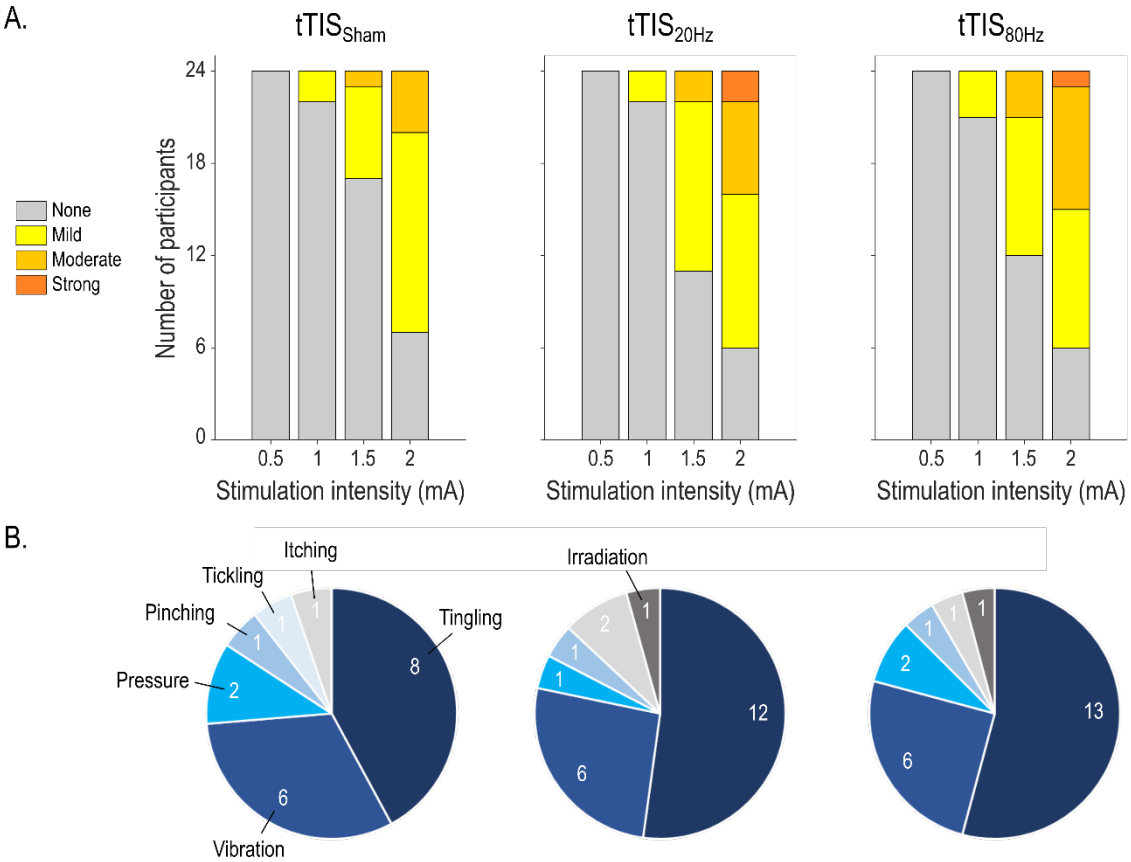

Figure S5. tTIS-related sensations. A) Magnitude of tTIS-related sensations. Magnitude of sensations reported before the experiment for current amplitudes ranging from 0.5 to 2 mA for each tTIS$_{TYPE}$. The current amplitude used in the present experiment was 2 mA. **B) Types of tTIS-related sensations.** Type of sensations as described by the participants, at 2 mA. Note that subjects were allowed to describe their sensations with up to two different words.

9. Brain activity during reinforcement motor learning

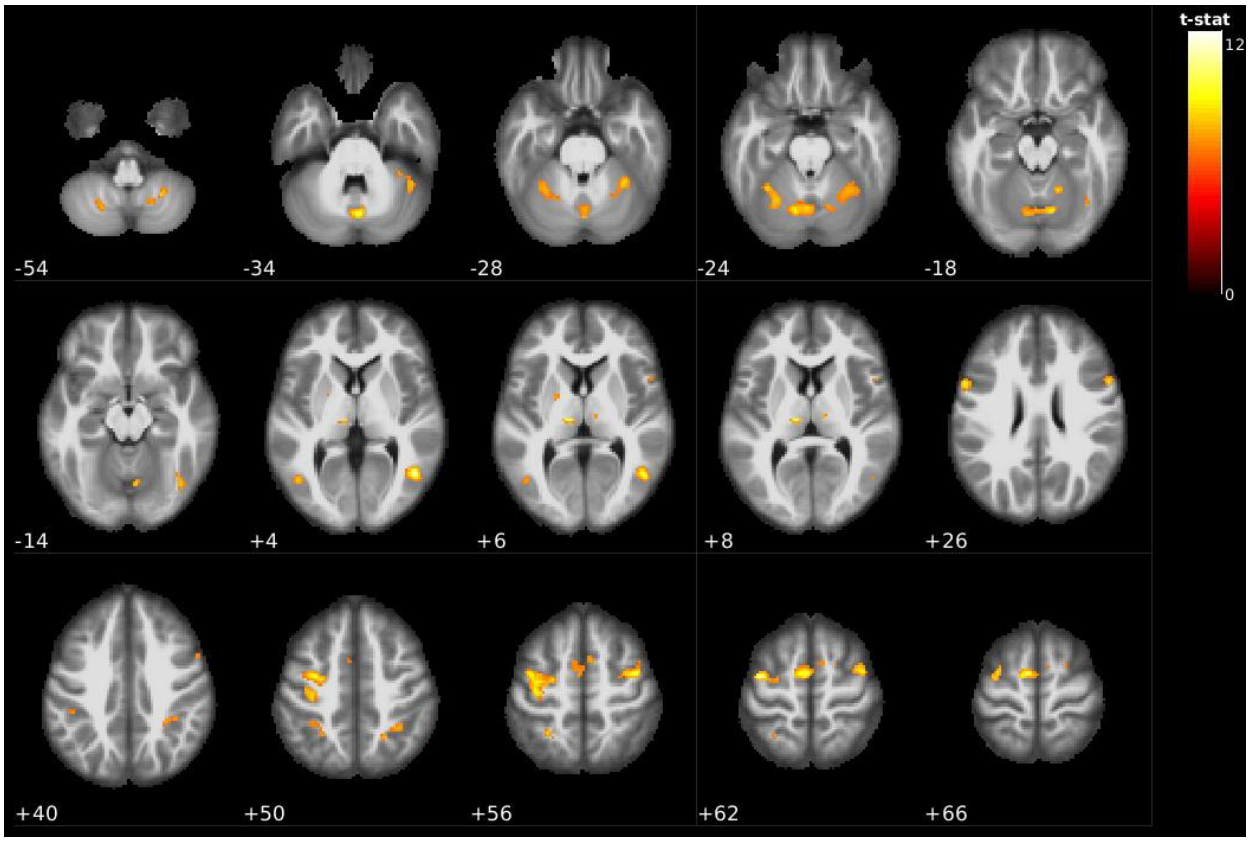

Figure S6. Whole-brain activity during reinforcement motor learning. Activation maps for the contrast task>rest in the $tTIS_{Sham}$, $Reinf_{ON}$ condition showing activation of key areas of the reinforcement motor learning network including the putamen, thalamus, cerebellum and sensorimotor network, especially on the left side. Significant clusters are shown for corrected voxel-wise family wise error (FWE), p=0.05, and corrected cluster-based false discovery rate (FDR), p=0.05.

Cluster-level				Peak-level					x	y	z	Region
$p_{FWE-corr}$	$q_{FDR-corr}$	k_E	P_{uncorr}	$p_{FWE-corr}$	$q_{FDR-corr}$	T	(Z_E)	P_{uncorr}				
<0.001	<0.001	135	<0.001	<0.001	0.005	12.63	6.84	<0.001	46	-62	4	Temporal_Mid_R
<0.001	<0.001	523	<0.001	<0.001	0.005	12.32	6.77	<0.001	-40	-8	62	Precentral_L
				<0.001	0.021	10.62	6.33	<0.001	-34	-6	52	Postcentral_L
				<0.001	0.021	10.43	6.28	<0.001	-36	-20	54	Precentral_L
<0.001	<0.001	335	<0.001	<0.001	0.018	11.08	6.46	<0.001	-8	-6	64	Supp_Motor_Area_L
				0.003	0.145	8.21	5.56	<0.001	6	6	58	Supp_Motor_Area_R
				0.003	0.145	8.20	5.55	<0.001	-4	-2	54	Supp_Motor_Area_L
<0.001	<0.001	44	<0.001	<0.001	0.021	10.65	6.34	<0.001	-10	-20	6	Thal_IL_L
<0.001	<0.001	162	<0.001	<0.001	0.021	10.36	6.26	<0.001	42	-6	56	Frontal_Mid_2_R
				<0.001	0.042	9.48	5.99	<0.001	34	-4	58	Frontal_Sup_2_R
<0.001	<0.001	175	<0.001	<0.001	0.021	10.27	6.23	<0.001	-58	10	28	Precentral_L
				<0.001	0.037	9.60	6.03	<0.001	-56	8	20	Frontal_Inf_Oper_L
				0.019	0.490	7.32	5.21	<0.001	-48	2	16	Rolandic_Oper_L
<0.001	<0.001	601	<0.001	<0.001	0.024	10.06	6.17	<0.001	2	-74	-34	Vermis_7
				<0.001	0.025	9.99	6.15	<0.001	-12	-70	-22	Cerebellum_6_L
				<0.001	0.027	9.88	6.12	<0.001	12	-70	-20	Cerebellum_6_R
<0.001	<0.001	82	<0.001	<0.001	0.070	9.14	5.88	<0.001	56	10	26	Frontal_Inf_Oper_R
				0.006	0.234	7.86	5.42	<0.001	56	10	38	Precentral_R
<0.001	<0.001	141	<0.001	0.001	0.092	8.89	5.80	<0.001	-34	-52	-24	Cerebellum_6_L
				0.002	0.117	8.47	5.65	<0.001	-28	-62	-24	Cerebellum_6_L
<0.001	<0.001	76	<0.001	0.001	0.092	8.87	5.79	<0.001	-28	-52	56	Parietal_Sup_L
				0.011	0.341	7.57	5.31	<0.001	-30	-44	48	Parietal_Inf_L
<0.001	<0.001	200	<0.001	0.001	0.092	8.77	5.76	<0.001	32	-48	-28	Cerebellum_6_R
				0.013	0.382	7.49	5.28	<0.001	34	-40	-34	Cerebellum_6_R
<0.001	<0.001	36	<0.001	0.001	0.092	8.73	5.74	<0.001	16	-54	-18	Cerebellum_4_5_R
<0.001	<0.001	28	<0.001	0.001	0.101	8.63	5.71	<0.001	26	-58	-54	Cerebellum_8_R
<0.001	<0.001	62	<0.001	0.001	0.113	8.51	5.67	<0.001	38	-62	-16	Fusiform_R
				0.002	0.117	8.45	5.64	<0.001	42	-72	-12	Occipital_Inf_R
<0.001	<0.001	21	<0.001	0.002	0.117	8.41	5.63	<0.001	-46	-68	4	Occipital_Mid_L
<0.001	<0.001	141	<0.001	0.002	0.130	8.33	5.60	<0.001	22	-56	50	Location not in atlas
				0.002	0.130	8.30	5.59	<0.001	30	-48	48	Parietal_Sup_R
				0.007	0.266	7.76	5.39	<0.001	36	-40	42	SupraMarginal_R
<0.001	<0.001	29	<0.001	0.004	0.170	8.09	5.51	<0.001	44	-50	-34	Cerebellum_Crus1_R

<0.001	<0.001	59	<0.001	0.004	0.178	8.04	5.49	<0.001	-22	-66	-52	Cerebellum_8_L
<0.001	0.006	12	0.003	0.004	0.190	7.99	5.47	<0.001	10	-16	8	Thal_MDl_R
0.001	0.043	6	0.028	0.009	0.319	7.63	5.33	<0.001	-22	-2	6	Putamen_L
<0.001	<0.001	34	<0.001	0.009	0.319	7.63	5.33	<0.001	18	-64	-54	Cerebellum_8_R
0.001	0.300	7	0.019	0.023	0.545	7.23	5.17	<0.001	20	2	62	Frontal_Sup_2_R
0.001	0.030	7	0.019	0.024	0.560	7.21	5.16	<0.001	52	12	8	Frontal_Inf_Oper_R
0.001	0.030	7	0.019	0.025	0.568	7.19	5.16	<0.001	-44	-36	40	Parietal_Inf_L

Table S2: Significant clusters and the respective local maxima in the $tTIS_{Sham}$, $Reinf_{ON}$ condition. Related to Figure S6. Regions were identified with the Automated Anatomical Labelling atlas 3 (AAL3[139]). Significant clusters were selected for corrected voxel-wise family wise error (FWE), p=0.05, and corrected cluster-based false discovery rate (FDR), p=0.05.

10. Correlation between effect of $tTIS_{80Hz}$ on reinforcement motor learning and modulation of whole-brain activity

Cluster-level				Peak-level					x	y	z	Region
$p_{FWE-corr}$	$q_{FDR-corr}$	k_E	P_{uncorr}	$p_{FWE-corr}$	$q_{FDR-corr}$	T	(Z_E)	P_{uncorr}				
0.003	**0.005**	**157**	**<0.001**	**0.027**	**0.065**	**7.29**	**5.14**	**<0.001**	**10**	**18**	**0**	Caudate_R
				0.639	0.678	5.38	4.25	<0.001	0	0	10	Location not in atlas
				0.921	0.757	4.89	3.98	<0.001	6	6	2	Location not in atlas
0.007	**0.005**	**138**	**<0.001**	**0.693**	**0.678**	**5.30**	**4.21**	**<0.001**	**-16**	**14**	**6**	Location not in atlas
				0.923	0.757	4.88	3.98	<0.001	-22	14	-2	Putamen_L
				1.000	0.810	4.26	3.60	<0.001	-18	8	-6	Putamen_L

Table S3. Significant clusters for the correlation between the behavioural and neural effects of $tTIS_{80Hz}$ (vs. $tTIS_{20Hz}$). Related to Figure 3B. Two significant clusters were found with several local maxima. Notably, the left cluster also encompassed a portion of the left caudate (related to Figure 3). Regions were identified with the Automated Anatomical Labelling atlas 3 (AAL3[139]). Significant clusters were selected for uncorrected voxel-wise family wise error (FWE), p=0.001, and corrected cluster-based false discovery rate (FDR), p=0.05.

11. Control analysis on striatum to frontal cortex effective connectivity

The connectivity analysis showed that $tTIS_{80Hz}$, but not $tTIS_{20Hz}$, increased striatum to frontal effective connectivity and that this effect depended on the type of network considered

(reward vs. motor) and on the presence of reinforcement (Figure 4). In this analysis we considered effective connectivity between the motor striatum and M1 and SMA for the motor network and the limbic striatum with ACC and vmPFC for the reward network, based on a large body of literature[11,12,135,136] (see Methods for a detailed justification of the ROIs). To verify whether our results depended on the specific frontal ROIs included in the analysis, we performed a new analysis. More specifically, we decomposed connectivity in each network for each frontal cortical area (M1 and SMA in the motor network and ACC and vmPFC in the reward network) and ran two separate LMMs on each network with $tTIS_{TYPE}$, $Reinf_{TYPE}$ as well as ROI_{TYPE} (M1 or SMA for the LMM run on the motor network and ACC or vmPFC for the reward network) as fixed effects. Consistent with our initial findings, we found effects of $tTIS_{TYPE}$ on both LMMs (motor network: $F_{(2,1089.7)}=3.12$; $p=0.044$ and reward network: $F_{(2,1112)}=6.78$; $p=0.0012$). Moreover, there was a significant $tTIS_{TYPE}$ x $Reinf_{TYPE}$ interaction in the motor network ($F_{(2,1112)}=3.36$; $p=0.035$), which was at the trend level in the reward network ($F_{(2,1113.8)}=2.37$; $p=0.094$). Most importantly, these effects were not modulated by ROI_{TYPE} in any network ($tTIS_{TYPE}$ x $Reinf_{TYPE}$ x ROI_{TYPE} in motor network: $F_{(2,1112)}=0.83$; $p=0.44$, in reward network: $F_{(2,1112)}=0.61$; $p=0.54$). This analysis suggests that the main connectivity findings were not influenced by the specific frontal ROIs considered in the analysis.

12. Relationship between the neural and behavioural effects of $tTIS_{80Hz}$ and impulsivity

Characterising individual factors that influence responsiveness to brain stimulation is an important line of research both for fundamental neuroscience but also to determine profiles of responders for future clinical translation. Based on previous literature linking striatal gamma oscillatory mechanisms and impulsivity[72], we explored the possibility that impulsivity influences responsiveness to striatal $tTIS_{80Hz}$ (**Figure S7**).

First, we exploited the BOLD data and asked if inter-individual variability in the neural effects of $tTIS_{80Hz}$ during reinforcement motor learning (i.e., in the $Reinf_{ON}$ condition) was related to impulsivity at the whole-brain level. Impulsivity was evaluated by a well-established independent delay-discounting questionnaire performed at the beginning of the experiment[75,76]. Strikingly, this analysis revealed that impulsivity was associated to the effect of $tTIS_{80Hz}$ (with respect to $tTIS_{20Hz}$) specifically in the left caudate nucleus (Figure S7A, Table S4). No other clusters were found. As such, the most impulsive participants exhibited an increase of left caudate activity with $tTIS_{80Hz}$ (compared to $tTIS_{20Hz}$) while the least impulsive ones rather presented a decrease of BOLD signal, consistent with the idea that impulsivity modulates the neuronal responsiveness to tTIS (R^2=0.47; $p<0.001$; Figure S7B). No significant clusters of correlation were found for the $tTIS_{80Hz}$ – $tTIS_{Sham}$ contrast, neither for the control $tTIS_{20Hz}$ - $tTIS_{Sham}$ contrast. Hence, this analysis suggests that the effect of $tTIS_{80Hz}$ on caudate activity depends on participants' impulsivity.

As a second step, we aimed at evaluating the association between impulsivity and the increased striatum to motor cortex connectivity observed with $tTIS_{80Hz}$, in the presence of reinforcement. Notably, such pattern of increased connectivity in fronto-striatal circuits has been described as a pathophysiological mechanism in multiple neuro-psychiatric disorders involving impulsivity[101–104]. Hence, we first asked if striatum to motor cortex connectivity was related to impulsivity during reinforcement motor learning in the absence of stimulation (i.e., in the $tTIS_{Sham}$ condition). Indeed, we found a significant positive relationship between impulsivity and striatum to motor cortex connectivity (robust linear regression: R^2=0.10; p=0.0038), in line with previous results[101–104]. Then, we evaluated whether the increase of connectivity observed with $tTIS_{80Hz}$ in the $Reinf_{ON}$ condition (Figure 4A) could be related to impulsivity. Indeed, we found that the effect of $tTIS_{80Hz}$ on connectivity was negatively correlated to impulsivity both when contrasting $tTIS_{80Hz}$ with $tTIS_{Sham}$ (R^2=0.19; p=0.043, Figure S7C, left) and with $tTIS_{20Hz}$ (R^2=0.28; p=0.021, Figure S7C, middle): participants with the largest increase in connectivity with $tTIS_{80Hz}$ in the $Reinf_{ON}$ condition

were also the least impulsive ones. Such correlation was absent when contrasting $tTIS_{20Hz}$ and $tTIS_{Sham}$ (R^2=0.0031; p=0.31, Figure S7C, right), but also when considering the same contrasts in the reward instead of the motor network (p=0.93 and p=0.86 for the $tTIS_{80Hz}$-$tTIS_{Sham}$ and $tTIS_{80Hz}$-$tTIS_{20Hz}$ contrasts, respectively). Hence, striatum to motor cortex effective connectivity during the task was positively correlated to impulsivity, but the change in connectivity induced by $tTIS_{80Hz}$ was rather negatively associated with impulsivity. This may be due to a ceiling effect in the most impulsive participants: exhibiting initially high levels of connectivity may leave less room for further modulation by $tTIS_{80Hz}$. These results suggest that inter-individual variability in impulsivity might influence neural responses to striatal $tTIS_{80Hz}$.

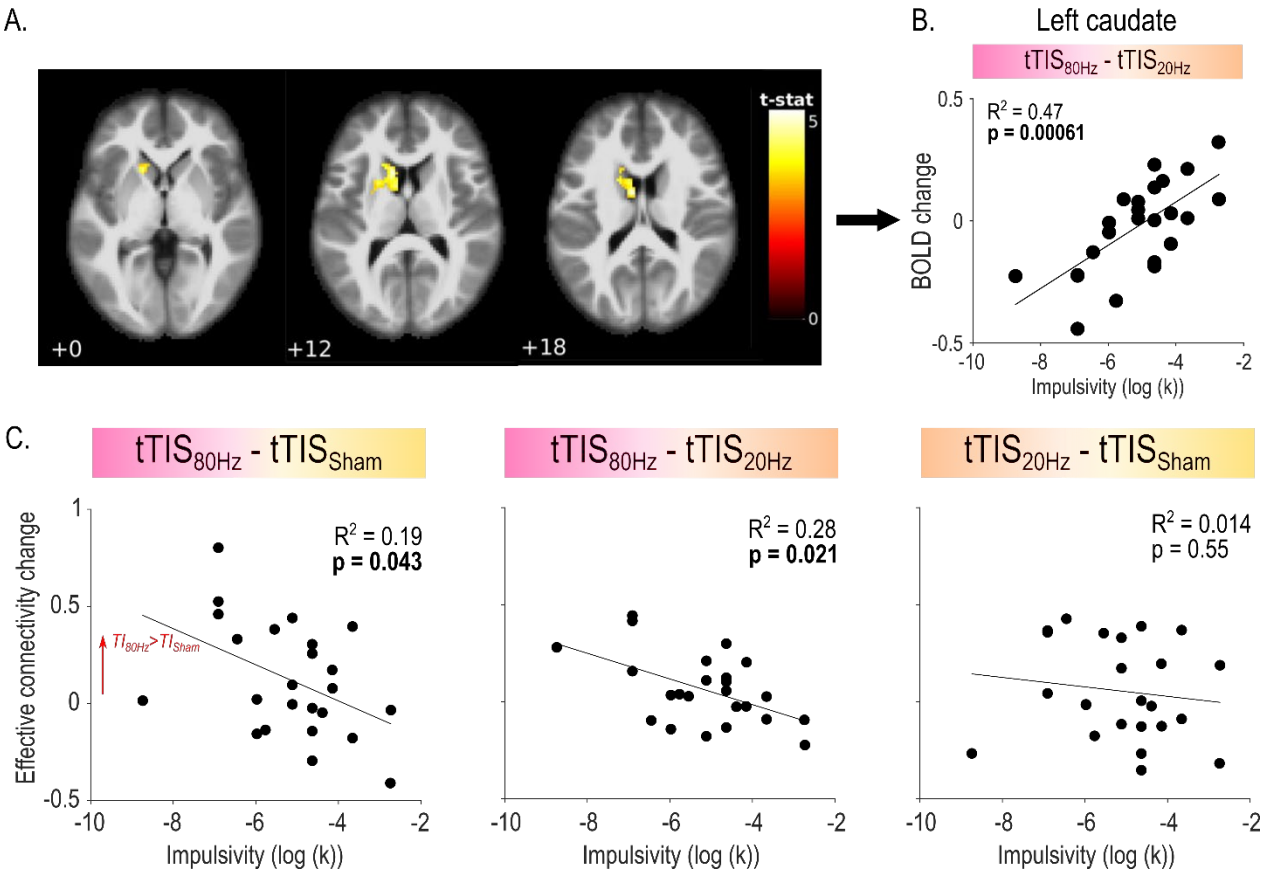

Figure S7. Relationship between impulsivity and the neural effects of $tTIS_{80Hz}$. A) Whole-brain correlation between the neural effects of $tTIS_{80Hz}$ (with respect to $tTIS_{20Hz}$) and impulsivity. Correlation between tTIS-related modulation of striatal activity ($tTIS_{80Hz}$ – $tTIS_{20Hz}$) during reinforcement motor learning ($Reinf_{ON}$) and individual impulsivity levels. A single significant cluster of correlation was found in left caudate (uncorrected voxel-wise FWE: p=0.001, and

corrected cluster-based FDR: p=0.05). **B) Correlation between left caudate activity and impulsivity.** A positive correlation was found showing that participants with higher levels of impulsivity exhibited stronger activation of the left caudate in the $tTIS_{80Hz}$ (with respect to $tTIS_{20Hz}$). **C) Correlations between impulsivity and tTIS-related modulation of effective connectivity.** Impulsivity was associated to the neural effects of $tTIS_{80Hz}$ both when contrasting to $tTIS_{Sham}$ (left) and $tTIS_{20Hz}$ (middle), but was not correlated to the effect of $tTIS_{20Hz}$ (right).

Cluster-level				Peak-level					x	y	z	Region
$p_{FWE-corr}$	$q_{FDR-corr}$	k_E	P_{uncorr}	$p_{FWE-corr}$	$q_{FDR-corr}$	T	(Z_E)	P_{uncorr}				
<0.001	**<0.001**	**254**	**<0.001**	**0.707**	**0.524**	**5.29**	**4.20**	**<0.001**	**-8**	**0**	**18**	Location not in atlas
				0.719	0.524	5.27	4.19	<0.001	-14	16	16	Caudate_L
				0.971	0.620	4.72	3.88	<0.001	-16	16	0	Location not in atlas

Table S4. Significant clusters for the correlation between impulsivity and effects of $tTIS_{80Hz}$ on BOLD activity (vs. $tTIS_{20Hz}$). Related to Figure S7A. One significant cluster encompassing the left caudate nucleus was found. Regions were identified with AAL3[139].

As a last step, we verified if impulsivity was also predictive of the behavioural effects of $tTIS_{80Hz}$ on reinforcement motor learning. We did not find any significant correlation between impulsivity and the effect of $tTIS_{80Hz}$ on motor learning ($tTIS_{80Hz}$ – $tTIS_{Sham}$: R^2=0.098; p=0.17; $tTIS_{80Hz}$ – $tTIS_{20Hz}$: R^2=0.11; p=0.21). Hence, impulsivity was associated to the neural, but not the behavioural effects of $tTIS_{80Hz}$.

Overall, we found that impulsivity was associated to $tTIS_{80Hz}$-related BOLD changes specifically in the left caudate and to changes of effective connectivity between the motor striatum and motor cortex during reinforcement motor learning. Hence, a possibility is that the differences in endogenous striatal gamma-related activity that have been associated to impulsive behaviour in animal models[72–74], influence the neural effects of $tTIS_{80Hz}$. If this is the case, impulsivity could constitute a behavioural factor allowing to determine responsiveness to striatal $tTIS_{80Hz}$.

Conversely, an interesting avenue for future research could aim at determining whether impulsivity can be modulated by striatal $tTIS_{80Hz}$.

13. Imaging quality control

A threshold of 0.5 was chosen to discard subjects showing more than 40% of voxels with framewise displacement FD higher than this threshold. In the current study cohort, no subject exceeded the limit value, thus the whole dataset could be used. Furthermore, successful cleaning of the data was ensured by visual checking the preprocessing results. In particular, good registration between anatomical and functional images and normalization to standard space were checked. Signal to noise ratio analysis showed significantly higher tSNR values underneath the stimulating electrodes ($F_{(1,1122)}=249.25$, $p<0.001$; **Figure S5**). Moreover, an additional analysis showed that this effect was not influenced by the $tTIS_{TYPE}$ ($Sphere_{LOCATION}$ x $tTIS_{TYPE}$: $F_{(2,1118)}=0.0169$, $p=0.98$). This result suggests that the stimulation did not introduce additional noise to the MR images. In summary, all controls confirmed the good quality of the imaging data.

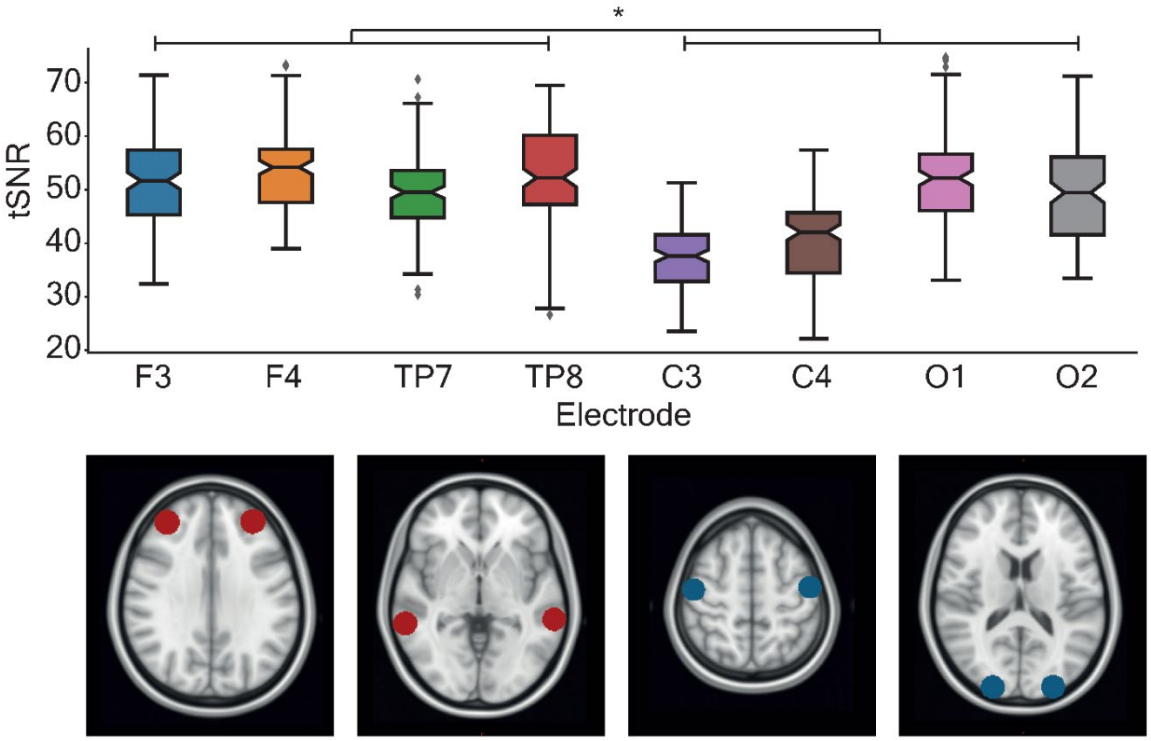

Figure S8. Total signal to noise ratio (tSNR). Total signal to noise ratio investigation. On the top panel, the average tSNR is shown within spheres of 10mm radius underneath the 4 stimulation electrodes (F3, F4, TP7 and TP8) and underneath other 4 locations more distal from the electrodes (C3, C4, O1 and O2). A significant higher tSNR was found underneath the electrodes with respect to the distal locations ($F_{(1,1122)}=249.25$, $p<0.001$). This indicates that there was no reduction of the tSNR due to the presence of electrical current. On the bottom panel, the location of the spheres from where the average tSNRs were extracted: F3 and F4 in red in the first image from the left, TP7 and TP8 in red on the second image from the left, C3 and C4 in blue on the third image from the left, O1 and O2 in blue on the forth image from the left.

Acknowledgements

P.V. was a PhD student supported by the Fund for Research training in Industry and Agriculture (FRIA/FNRS; FC29690), and grants by the Platform for Education and Talent (Gustave Boël - Sofina Fellowships) and Wallonie-Bruxelles International. J.D. was supported by grants from the Belgian FNRS and the Fondation Médicale Reine Elisabeth (FMRE). G.D. was supported by the Belgian FNRS. The research was partially funded by the Novartis Research Foundation—FreeNovation (Basel, CH) to MJW and EN, the Bertarelli Foundation (Catalyst 'Deep-MCI-T', Gstaad, CH) to FCH, the SNSF Lead Agency (NiBS-iCog 320030L_197899) to FCH and the Defitech Foundation (Morges, CH) to FCH. We acknowledge access to and expertise of the Neuromodulation and the Neuroimaging facilities of the Human Neuroscience Platform of the Campus Biotech Geneva and of the MRI Platform of the HVS (Sion). We would also like to thank Prof. Leonardo Cohen for insightful feedback on a previous version of this manuscript.

Competing interests

E.N. is co-founder of TI Solutions AG, a company committed to producing hardware and software solutions to support tTIS research.

Data and code availability statement

The datasets generated during the current study and the code used to analyse them are available from the corresponding author on reasonable request.

1380 **References**

1381 1. Neftci, E. O. & Averbeck, B. B. Reinforcement learning in artificial and biological
1382 systems. *Nat. Mach. Intell.* **1**, 133–143 (2019).

1383 2. Schultz, W. Neuronal Reward and Decision Signals: From Theories to Data.
1384 *Physiol. Rev.* **95**, 853–951 (2015).

1385 3. Dhawale, A. K., Smith, M. A. & Ölveczky, B. P. The Role of Variability in Motor
1386 Learning. *Annu. Rev. Neurosci.* **40**, 479–498 (2017).

1387 4. Vassiliadis, P. *et al.* Reward boosts reinforcement-based motor learning. *iScience*
1388 **24**, 102821 (2021).

1389 5. Spampinato, D. & Celnik, P. Multiple Motor Learning Processes in Humans:
1390 Defining Their Neurophysiological Bases. *Neuroscientist* **27**, 246–267 (2021).

1391 6. Huang, V. S., Haith, A., Mazzoni, P. & Krakauer, J. W. Rethinking Motor Learning
1392 and Savings in Adaptation Paradigms: Model-Free Memory for Successful Actions
1393 Combines with Internal Models. *Neuron* **70**, 787–801 (2011).

1394 7. Galea, J. M., Mallia, E., Rothwell, J. & Diedrichsen, J. The dissociable effects of
1395 punishment and reward on motor learning. *Nat. Neurosci.* **18**, 597–602 (2015).

1396 8. Therrien, A. S., Wolpert, D. M. & Bastian, A. J. Effective Reinforcement learning
1397 following cerebellar damage requires a balance between exploration and motor
1398 noise. *Brain* **139**, 101–114 (2016).

1399 9. Vassiliadis, P., Derosiere, G. & Duque, J. Beyond Motor Noise : Considering Other
1400 Causes of Impaired Reinforcement Learning in Cerebellar Patients. *Eneuro* **6**, 1–4
1401 (2019).

1402 10. Widmer, M. *et al.* Reward During Arm Training Improves Impairment and Activity
1403 After Stroke: A Randomized Controlled Trial. *Neurorehabil. Neural Repair* **0**,
1404 154596832110628 (2021).

1405 11. Bartra, O., McGuire, J. T. & Kable, J. W. The valuation system: A coordinate-
1406 based meta-analysis of BOLD fMRI experiments examining neural correlates of
1407 subjective value. *Neuroimage* **76**, 412–427 (2013).

1408 12. Hardwick, R. M., Rottschy, C., Miall, R. C. & Eickhoff, S. B. A quantitative meta-
1409 analysis and review of motor learning in the human brain. *Neuroimage* **67**, 283–
1410 297 (2013).

1411 13. Haber, S. N. Corticostriatal circuitry. *Dialogues Clin. Neurosci.* **18**, 7–21 (2016).

1412 14. Balleine, B. W., Delgado, M. R. & Hikosaka, O. The role of the dorsal striatum in
1413 reward and decision-making. *J. Neurosci.* **27**, 8161–8165 (2007).

1414 15. Piray, P., den Ouden, H. E. M., van der Schaaf, M. E., Toni, I. & Cools, R.
1415 Dopaminergic modulation of the functional ventrodorsal architecture of the human
1416 striatum. *Cereb. Cortex* **27**, 485–495 (2017).

1417 16. Hori, Y. *et al.* Ventral striatum links motivational and motor networks during
1418 operant-conditioned movement in rats. *Neuroimage* **184**, 943–953 (2019).

1419 17. Wachter, T., Lungu, O. V., Liu, T., Willingham, D. T. & Ashe, J. Differential Effect
1420 of Reward and Punishment on Procedural Learning. *J. Neurosci.* **29**, 436–443
1421 (2009).

1422 18. Widmer, M., Ziegler, N., Held, J., Luft, A. & Lutz, K. Rewarding feedback promotes
1423 motor skill consolidation via striatal activity. in *Progress in Brain Research* **5**, 303–

323 (2016).

19. Berke, J. D. Fast oscillations in cortical-striatal networks switch frequency following rewarding events and stimulant drugs. *Eur. J. Neurosci.* **30**, 848–859 (2009).

20. van der Meer, M. A. A. *et al.* Integrating early results on ventral striatal gamma oscillations in the rat. *Front. Neurosci.* **4**, 1–12 (2010).

21. van der Meer, M. A. A. & Redish, A. D. Low and high gamma oscillations in rat ventral striatum have distinct relationships to behavior, reward, and spiking activity on a learned spatial decision task. *Front. Integr. Neurosci.* **3**, 1–19 (2009).

22. Dwiel, L. L., Khokhar, J. Y., Connerney, M. A., Green, A. I. & Doucette, W. T. Finding the balance between model complexity and performance: Using ventral striatal oscillations to classify feeding behavior in rats. *PLoS Comput. Biol.* **15**, 1–19 (2019).

23. Matsumoto, J. *et al.* Neuronal responses in the nucleus accumbens shell during sexual behavior in male rats. *J. Neurosci.* **32**, 1672–1686 (2012).

24. Kalenscher, T., Lansink, C. S., Lankelma, J. V. & Pennartz, C. M. A. Reward-associated gamma oscillations in ventral striatum are regionally differentiated and modulate local firing activity. *J. Neurophysiol.* **103**, 1658–1672 (2010).

25. Cohen, M. X. *et al.* Good vibrations: Cross-frequency coupling in the human nucleus accumbens during reward processing. *J. Cogn. Neurosci.* **21**, 875–889 (2009).

26. Sepe-Forrest, L., Carver, F. W., Quentin, R., Holroyd, T. & Nugent, A. C. Basal

1446 ganglia activation localized in MEG using a reward task. *Neuroimage: Reports* **1**,
1447 100034 (2021).

1448 27. Herrojo-Ruiz, M. *et al.* Involvement of human internal globus pallidus in the early
1449 modulation of cortical error-related activity. *Cereb. Cortex* **24**, 1502–1517 (2014).

1450 28. Jenkinson, N. & Brown, P. New insights into the relationship between dopamine,
1451 beta oscillations and motor function. *Trends Neurosci.* **34**, 611–618 (2011).

1452 29. Brown, P. Abnormal oscillatory synchronisation in the motor system leads to
1453 impaired movement. *Curr. Opin. Neurobiol.* **17**, 656–664 (2007).

1454 30. McCarthy, M. M. *et al.* Striatal origin of the pathologic beta oscillations in
1455 Parkinson's disease. *Proc. Natl. Acad. Sci. U. S. A.* **108**, 11620–11625 (2011).

1456 31. Kondabolu, K. *et al.* Striatal cholinergic interneurons generate beta and gamma
1457 oscillations in the corticostriatal circuit and produce motor deficits. *Proc. Natl.*
1458 *Acad. Sci. U. S. A.* **113**, 3159–3168 (2016).

1459 32. Silberstein, P. *et al.* Cortico-cortical coupling in Parkinson's disease and its
1460 modulation by therapy. *Brain* **128**, 1277–1291 (2005).

1461 33. Williams, Z. M. & Eskandar, E. N. Selective enhancement of associative learning
1462 by microstimulation of the anterior caudate. *Nat. Neurosci.* **9**, 562–568 (2006).

1463 34. Nakamura, K. & Hikosaka, O. Facilitation of saccadic eye movements by
1464 postsaccadic electrical stimulation in the primate caudate. *J. Neurosci.* **26**, 12885–
1465 12895 (2006).

1466 35. Deng, Z. De, Lisanby, S. H. & Peterchev, A. V. Electric field depth-focality tradeoff
1467 in transcranial magnetic stimulation: Simulation comparison of 50 coil designs.

1468 *Brain Stimul.* **6**, 1–13 (2013).

1469 36. Wagner, T. *et al.* Transcranial direct current stimulation: A computer-based human
1470 model study. *Neuroimage* **35**, 1113–1124 (2007).

1471 37. Nickchen, K. *et al.* Reversal learning reveals cognitive deficits and altered
1472 prediction error encoding in the ventral striatum in Huntington's disease. *Brain*
1473 *Imaging Behav.* **11**, 1862–1872 (2017).

1474 38. Schmidt, L. *et al.* Disconnecting force from money: Effects of basal ganglia
1475 damage on incentive motivation. *Brain* **131**, 1303–1310 (2008).

1476 39. Seymour, B. *et al.* Deep brain stimulation of the subthalamic nucleus modulates
1477 sensitivity to decision outcome value in Parkinson's disease. *Sci. Rep.* **6**, 1–12
1478 (2016).

1479 40. Atkinson-Clement, C. *et al.* Effects of subthalamic nucleus stimulation and
1480 levodopa on decision-making in Parkinson's disease. *Mov. Disord.* **34**, 377–385
1481 (2019).

1482 41. Grossman, N. *et al.* Noninvasive Deep Brain Stimulation via Temporally Interfering
1483 Electric Fields. *Cell* **169**, 1029-1041.e16 (2017).

1484 42. Song, S., Zhang, J., Tian, Y., Wang, L. & Wei, P. Temporal Interference
1485 Stimulation Regulates Eye Movements and Neural Activity in the Mice Superior
1486 Colliculus. *Proc. Annu. Int. Conf. IEEE Eng. Med. Biol. Soc. EMBS* 6231–6234
1487 (2021). doi:10.1109/EMBC46164.2021.9629968

1488 43. Esmaeilpour, Z., Kronberg, G., Reato, D., Parra, L. C. & Bikson, M. Temporal
1489 interference stimulation targets deep brain regions by modulating neural

1490 oscillations. *Brain Stimul.* **14**, 55–65 (2021).

1491 44. Rampersad, S. *et al.* Prospects for transcranial temporal interference stimulation
1492 in humans: A computational study. *Neuroimage* **202**, 116124 (2019).

1493 45. von Conta, J. *et al.* Interindividual variability of electric fields during transcranial
1494 temporal interference stimulation (tTIS). *Sci. Rep.* **11**, 1–12 (2021).

1495 46. Cao, J., Doiron, B., Goswami, C. & Grover, P. The mechanics of temporal
1496 interference stimulation. *bioRxiv* 1–6 (2020). doi:10.1101/2020.04.23.051870

1497 47. Mirzakhalili, E., Barra, B., Capogrosso, M. & Lempka, S. F. Biophysics of
1498 Temporal Interference Stimulation. *Cell Syst.* **11**, 557-572.e5 (2020).

1499 48. von Conta, J. *et al.* Benchmarking the effects of transcranial temporal interference
1500 stimulation (tTIS) in humans. *Cortex* **154**, 299–310 (2022).

1501 49. Ma, R. *et al.* High Gamma and Beta Temporal Interference Stimulation in the
1502 Human Motor Cortex Improves Motor Functions. *Front. Neurosci.* **15**, 1–11 (2022).

1503 50. Hutcheon, B. & Yarom, Y. Resonance, oscillation and the intrinsic frequency
1504 preferences of neurons. *Trends Neurosci.* **23**, 216–222 (2000).

1505 51. Acerbo, E. *et al.* Focal non-invasive deep-brain stimulation with temporal
1506 interference for the suppression of epileptic biomarkers. *Front. Neurosci.* **16**, 1–12
1507 (2022).

1508 52. Wessel, M. J. *et al.* LTP-like noninvasive striatal brain stimulation enhances
1509 striatal activity and motor skill learning in humans. *bioRxiv* 1–30 (2022).
1510 doi:10.1101/2022.10.28.514204

1511 53. Violante, I. R. *et al.* Non-invasive temporal interference electrical stimulation of the

1512 human hippocampus. *biorXiv* (2022). doi:10.1101/2022.09.14.507625

1513 54. Abe, M. *et al.* Reward improves long-term retention of a motor memory through
1514 induction of offline memory gains. *Curr. Biol.* **21**, 557–562 (2011).

1515 55. Steel, A., Silson, E. H., Stagg, C. J. & Baker, C. I. The impact of reward and
1516 punishment on skill learning depends on task demands. *Sci. Rep.* **6**, 1–9 (2016).

1517 56. Vassiliadis, P., Lete, A., Duque, J. & Derosiere, G. Reward timing matters in motor
1518 learning. *iScience* **25**, 104290 (2022).

1519 57. Izawa, J. & Shadmehr, R. Learning from sensory and reward prediction errors
1520 during motor adaptation. *PLoS Comput. Biol.* **7**, 1–12 (2011).

1521 58. Mawase, F., Uehara, S., Bastian, A. J. & Celnik, P. Motor Learning Enhances
1522 Use-Dependent Plasticity. *J. Neurosci.* **37**, 2673–2685 (2017).

1523 59. Iacono, M. I. *et al.* MIDA: A multimodal imaging-based detailed anatomical model
1524 of the human head and neck. *PLoS One* **10**, (2015).

1525 60. Jiang, T. Brainnetome: A new -ome to understand the brain and its disorders.
1526 *Neuroimage* **80**, 263–272 (2013).

1527 61. Areshenkoff, C. N., de Brouwer, A. J., Gale, D. J., Nashed, J. Y. & Gallivan, J. P.
1528 Separate and shared low-dimensional neural architectures for error-based and
1529 reinforcement motor learning. *biorXiv* (2022). doi:10.1101/2022.08.16.504134

1530 62. Cashaback, J. G. A., McGregor, H. R., Mohatarem, A. & Gribble, P. L.
1531 Dissociating error-based and reinforcement-based loss functions during
1532 sensorimotor learning. *PLoS Comput. Biol.* **13**, 1–28 (2017).

1533 63. Floyer-Lea, A. & Matthews, P. M. Changing brain networks for visuomotor control

1534 with increased movement automaticity. *J. Neurophysiol.* **92**, 2405–2412 (2004).

1535 64. Floyer-Lea, A. & Matthews, P. M. Distinguishable brain activation networks for
1536 short- and long-term motor skill learning. *J. Neurophysiol.* **94**, 512–518 (2005).

1537 65. Graybiel, A. M. & Grafton, S. T. The striatum: Where skills and habits meet. *Cold*
1538 *Spring Harb. Perspect. Biol.* **7**, 1–14 (2015).

1539 66. McLaren, D. G., Ries, M. L., Xu, G. & Johnson, S. C. A generalized form of
1540 context-dependent psychophysiological interactions (gPPI): A comparison to
1541 standard approaches. *Neuroimage* **61**, 1277–1286 (2012).

1542 67. Codol, O., Holland, P. J., Manohar, S. G. & Galea, J. M. Reward-Based
1543 Improvements in Motor Control Are Driven by Multiple Error-Reducing
1544 Mechanisms. *J. Neurosci.* **40**, 3604–3620 (2020).

1545 68. Sidarta, A., Vahdat, S., Bernardi, N. F. & Ostry, D. J. Somatic and reinforcement-
1546 based plasticity in the initial stages of human motor learning. *J. Neurosci.* **36**,
1547 11682–11692 (2016).

1548 69. Krause, M. R., Vieira, P. G., Csorba, B. A., Pilly, P. K. & Pack, C. C. Transcranial
1549 alternating current stimulation entrains single-neuron activity in the primate brain.
1550 *Proc. Natl. Acad. Sci. U. S. A.* **116**, 5747–5755 (2019).

1551 70. Shirer, W. R., Ryali, S., Rykhlevskaia, E., Menon, V. & Greicius, M. D. Decoding
1552 subject-driven cognitive states with whole-brain connectivity patterns. *Cereb.*
1553 *Cortex* **22**, 158–165 (2012).

1554 71. Morishita, T. & Hummel, F. C. Non-invasive Brain Stimulation (NIBS) in Motor
1555 Recovery After Stroke: Concepts to Increase Efficacy. *Curr. Behav. Neurosci.*

1556 *Reports* **4**, 280–289 (2017).

1557 72. Donnelly, N. A. *et al.* Oscillatory activity in the medial prefrontal cortex and nucleus
1558 accumbens correlates with impulsivity and reward outcome. *PLoS One* **9**, 14–17
1559 (2014).

1560 73. Schall, T. A., Wright, W. J. & Dong, Y. Nucleus accumbens fast-spiking
1561 interneurons in motivational and addictive behaviors. *Mol. Psychiatry* **26**, 234–246
1562 (2021).

1563 74. Pisansky, M. T. *et al.* Nucleus Accumbens Fast-Spiking Interneurons Constrain
1564 Impulsive Action. *Biol. Psychiatry* **86**, 836–847 (2019).

1565 75. Kirby, K. N., Petry, N. M. & Bickel, W. K. Heroin addicts have higher discount rates
1566 for delayed rewards than non-drug-using controls. *J. Exp. Psychol. Gen.* **128**, 78–
1567 87 (1999).

1568 76. Mitchell, J. M., Fields, H. L., D'Esposito, M. & Boettiger, C. A. Impulsive
1569 responding in alcoholics. *Alcohol. Clin. Exp. Res.* **29**, 2158–2169 (2005).

1570 77. Catanese, J., Carmichael, J. E. & van der Meer, M. A. A. Low- and high-gamma
1571 oscillations deviate in opposite directions from zero-phase synchrony in the limbic
1572 corticostriatal loop. *J. Neurophysiol.* **116**, 5–17 (2016).

1573 78. Rothé, M., Quilodran, R., Sallet, J. & Procyk, E. Coordination of high gamma
1574 activity in anterior cingulate and lateral prefrontal cortical areas during adaptation.
1575 *J. Neurosci.* **31**, 11110–11117 (2011).

1576 79. Del Arco, A., Park, J., Wood, J., Kim, Y. & Moghaddam, B. Adaptive encoding of
1577 outcome prediction by prefrontal cortex ensembles supports behavioral flexibility.

1578 *J. Neurosci.* **37**, 8363–8373 (2017).

1579 80. Yoshimoto, A., Shibata, Y., Kudara, M., Ikegaya, Y. & Matsumoto, N.
1580 Enhancement of Motor Cortical Gamma Oscillations and Sniffing Activity by
1581 Medial Forebrain Bundle Stimulation Precedes Locomotion. *eNeuro* **9**, 1–14
1582 (2022).

1583 81. Grover, S., Nguyen, J. A., Viswanathan, V. & Reinhart, R. M. G. High-frequency
1584 neuromodulation improves obsessive–compulsive behavior. *Nat. Med.* **27**, 232–
1585 238 (2021).

1586 82. Krause, M. R., Vieira, P. G., Thivierge, J. P. & Pack, C. C. Brain stimulation
1587 competes with ongoing oscillations for control of spike timing in the primate brain.
1588 *PLoS Biol.* **20**, 1–27 (2022).

1589 83. Courtemanche, R., Fujii, N. & Graybiel, A. M. Synchronous, Focally Modulated β-
1590 Band Oscillations Characterize Local Field Potential Activity in the Striatum of
1591 Awake Behaving Monkeys. *J. Neurosci.* **23**, 11741–11752 (2003).

1592 84. Costa, R. M. *et al.* Rapid Alterations in Corticostriatal Ensemble Coordination
1593 during Acute Dopamine-Dependent Motor Dysfunction. *Neuron* **52**, 359–369
1594 (2006).

1595 85. Engel, A. K. & Fries, P. Beta-band oscillations-signalling the status quo? *Curr.*
1596 *Opin. Neurobiol.* **20**, 156–165 (2010).

1597 86. Uehara, S., Mawase, F. & Celnik, P. Learning similar actions by reinforcement or
1598 sensory-prediction errors rely on distinct physiological mechanisms. *Cereb. Cortex*
1599 **28**, 3478–3490 (2018).

1600 87. Mathis, M. W., Mathis, A. & Uchida, N. Somatosensory Cortex Plays an Essential
1601 Role in Forelimb Motor Adaptation in Mice. *Neuron* **93**, 1493-1503.e6 (2017).

1602 88. Brücke, C. *et al.* Scaling of movement is related to pallidal γ oscillations in patients
1603 with dystonia. *J. Neurosci.* **32**, 1008–1019 (2012).

1604 89. Soderstrom, N. C. & Bjork, R. A. Learning Versus Performance: An Integrative
1605 Review. *Perspect. Psychol. Sci.* **10**, 176–199 (2015).

1606 90. Spampinato, D. A., Satar, Z. & Rothwell, J. C. Combining reward and M1
1607 transcranial direct current stimulation enhances the retention of newly learnt
1608 sensorimotor mappings. *Brain Stimul.* 1–8 (2019). doi:10.1016/j.brs.2019.05.015

1609 91. Shmuelof, L. *et al.* Overcoming Motor 'Forgetting' Through Reinforcement Of
1610 Learned Actions. *J. Neurosci.* **32**, 14617-14621a (2012).

1611 92. Dhawale, A. K., Miyamoto, Y. R., Smith, M. A. & Ölveczky, B. P. Adaptive
1612 Regulation of Motor Variability. *Curr. Biol.* **29**, 3551-3562.e7 (2019).

1613 93. Carroll, T. J., McNamee, D., Ingram, J. N. & Wolpert, D. M. Rapid visuomotor
1614 responses reflect value-based decisions. *J. Neurosci.* **39**, 3906–3920 (2019).

1615 94. De Comite, A., Crevecoeur, F. & Lefèvre, P. Reward-Dependent Selection of
1616 Feedback Gains Impacts Rapid Motor Decisions. *Eneuro* **9**, ENEURO.0439-
1617 21.2022 (2022).

1618 95. Codol, O. *et al.* Sensorimotor feedback loops are selectively sensitive to reward.
1619 *Elife* **12**, 1–25 (2023).

1620 96. Krakauer, J. W., Hadjiosif, A. M., Xu, J., Wong, A. L. & Haith, A. M. Motor
1621 Learning. *Compr. Physiol.* **9**, 613–663 (2019).

1622 97. Quattrocchi, G. *et al.* Pharmacological Dopamine Manipulation Does Not Alter
1623 Reward-Based Improvements in Memory Retention during a Visuomotor
1624 Adaptation Task. *Eneuro* **5**, ENEURO.0453-17.2018 (2018).

1625 98. Johnson, L. *et al.* Dose-dependent effects of transcranial alternating current
1626 stimulation on spike timing in awake nonhuman primates. *Sci. Adv.* **6**, 1–9 (2020).

1627 99. Beliaeva, V., Savvateev, I., Zerbi, V. & Polania, R. Toward integrative approaches
1628 to study the causal role of neural oscillations via transcranial electrical stimulation.
1629 *Nat. Commun.* **12**, 1–12 (2021).

1630 100. Averbeck, B. & O'Doherty, J. P. Reinforcement-learning in fronto-striatal circuits.
1631 *Neuropsychopharmacology* **47**, 147–162 (2022).

1632 101. Ma, I. *et al.* Ventral striatal hyperconnectivity during rewarded interference control
1633 in adolescents with ADHD. *Cortex* **82**, 225–236 (2016).

1634 102. Wang, Q. *et al.* Dissociated neural substrates underlying impulsive choice and
1635 impulsive action. *Neuroimage* **134**, 540–549 (2016).

1636 103. Mosley, P. E. *et al.* The structural connectivity of discrete networks underlies
1637 impulsivity and gambling in Parkinson's disease. *Brain* **142**, 3917–3935 (2019).

1638 104. Hampton, W. H., Alm, K. H., Venkatraman, V., Nugiel, T. & Olson, I. R.
1639 Dissociable frontostriatal white matter connectivity underlies reward and motor
1640 impulsivity. *Neuroimage* **150**, 336–343 (2017).

1641 105. Negahbani, E., Kasten, F. H., Herrmann, C. S. & Fröhlich, F. Targeting alpha-band
1642 oscillations in a cortical model with amplitude-modulated high-frequency
1643 transcranial electric stimulation. *Neuroimage* **173**, 3–12 (2018).

1644 106. Cohen, J. *Statistical power analysis for the behavioral sciences*. *L. Erlbaum*
1645 *Associates* **13**, (1988).

1646 107. Hashemirad, F., Zoghi, M., Fitzgerald, P. B. & Jaberzadeh, S. The effect of anodal
1647 transcranial direct current stimulation on motor sequence learning in healthy
1648 individuals: A systematic review and meta-analysis. *Brain Cogn.* **102**, 1–12 (2016).

1649 108. Soutschek, A., Kang, P., Ruff, C. C., Hare, T. A. & Tobler, P. N. Brain Stimulation
1650 Over the Frontopolar Cortex Enhances Motivation to Exert Effort for Reward. *Biol.*
1651 *Psychiatry* **84**, 38–45 (2018).

1652 109. Wischnewski, M., Zerr, P. & Schutter, D. J. L. G. Effects of Theta Transcranial
1653 Alternating Current Stimulation Over the Frontal Cortex on Reversal Learning.
1654 *Brain Stimul.* **9**, 705–711 (2016).

1655 110. Guerra, A., López-Alonso, V., Cheeran, B. & Suppa, A. Variability in non-invasive
1656 brain stimulation studies: Reasons and results. *Neurosci. Lett.* **719**, 133330
1657 (2020).

1658 111. Cassarà, A. M. *et al.* Safety Recommendations for Temporal Interference
1659 Stimulation in the Brain. *bioRxiv* 1–69 (2022). doi:10.1101/2022.12.15.520077

1660 112. Oldfield, R. C. The assessment and analysis of handedness: The Edinburgh
1661 inventory. *Neuropsychologia* **9**, 97–113 (1971).

1662 113. Kaplan, B. A. *et al.* Automating Scoring of Delay Discounting for the 21- and 27-
1663 Item Monetary Choice Questionnaires. *Behav. Anal.* **39**, 293–304 (2016).

1664 114. Mitchell, M. R. & Potenza, M. N. Recent Insights into the Neurobiology of
1665 Impulsivity. *Curr. Addict. Reports* **1**, 309–319 (2014).

1666 115. Brainard, D. H. The Psychophysics Toolbox. *Spat. Vis.* **10**, 433–436 (1997).

1667 116. Pelli, D. G. The VideoToolbox software for visual psychophysics: transforming
1668 numbers into movies. *Spat. Vis.* **10**, 437–442 (1997).

1669 117. Dayan, E., Averbeck, B. B., Richmond, B. J. & Cohen, L. G. Stochastic
1670 reinforcement benefits skill acquisition. *Learn. Mem.* **21**, 140–142 (2014).

1671 118. Grossman, N. Modulation without surgical intervention. *Science (80-.).* **361**, 461–
1672 462 (2018).

1673 119. Antal, A. *et al.* Low intensity transcranial electric stimulation: Safety, ethical, legal
1674 regulatory and application guidelines. *Clin. Neurophysiol.* **128**, 1774–1809 (2017).

1675 120. Ekhtiari, H. *et al.* A checklist for assessing the methodological quality of concurrent
1676 tES-fMRI studies (ContES checklist): a consensus study and statement. *Nat.*
1677 *Protoc.* **17**, 596–617 (2022).

1678 121. Bossetti, C. A., Birdno, M. J. & Grill, W. M. Analysis of the quasi-static
1679 approximation for calculating potentials generated by neural stimulation. *J. Neural*
1680 *Eng.* **5**, 44–53 (2008).

1681 122. Hasgall, P. *et al.* "IT'IS Database for thermal and electromagnetic parameters of
1682 biological tissues," Version 4.1. (2022). doi:10.13099/VIP21000-04-1

1683 123. Seeck, M. *et al.* The standardized EEG electrode array of the IFCN. *Clin.*
1684 *Neurophysiol.* **128**, 2070–2077 (2017).

1685 124. Bates, D., Mächler, M., Bolker, B. M. & Walker, S. C. Fitting linear mixed-effects
1686 models using lme4. *J. Stat. Softw.* **67**, (2015).

1687 125. Ryu, E. Effects of skewness and kurtosis on normal-theory based maximum

likelihood test statistic in multilevel structural equation modeling. *Behav. Res. Methods* **43**, 1066–1074 (2011).

126. Nieuwenhuis, R., te Grotenhuis, M. & Pelzer, B. Influence.ME: Tools for detecting influential data in mixed effects models. *R J.* **4**, 38–47 (2012).

127. Luke, S. G. Evaluating significance in linear mixed-effects models in R. *Behav. Res. Methods* **49**, 1494–1502 (2017).

128. Searle, S. R., Speed, F. M. & Milliken, G. A. Population marginal means in the linear model: An alternative to least squares means. *Am. Stat.* **34**, 216–221 (1980).

129. Ben-Shachar, M., Lüdecke, D. & Makowski, D. effectsize: Estimation of Effect Size Indices and Standardized Parameters. *J. Open Source Softw.* **5**, 2815 (2020).

130. Derosière, G., Billot, M., Ward, E. T. & Perrey, S. Adaptations of motor neural structures' activity to lapses in attention. *Cereb. Cortex* **25**, 66–74 (2015).

131. Okamoto, M. *et al.* Three-dimensional probabilistic anatomical cranio-cerebral correlation via the international 10-20 system oriented for transcranial functional brain mapping. *Neuroimage* **21**, 99–111 (2004).

132. Di, X., Zhang, Z. & Biswal, B. B. Understanding psychophysiological interaction and its relations to beta series correlation. *Brain Imaging Behav.* **15**, 958–973 (2021).

133. Bowles, S. *et al.* Vagus nerve stimulation drives selective circuit modulation through cholinergic reinforcement. *Neuron* **110**, 2867-2885.e7 (2022).

134. Codol, O., Galea, J. M., Jalali, R. & Holland, P. J. Reward-driven enhancements in

1710 motor control are robust to TMS manipulation. *bioRxiv* 2020.01.12.903419 (2020).
1711 doi:10.1101/2020.01.12.903419

1712 135. Draganski, B. *et al.* Evidence for segregated and integrative connectivity patterns
1713 in the human basal ganglia. *J. Neurosci.* **28**, 7143–7152 (2008).

1714 136. Morris, L. S. *et al.* Fronto-striatal organization: Defining functional and
1715 microstructural substrates of behavioural flexibility. *Cortex* **74**, 118–133 (2016).

1716 137. Lam, S. Y. & Zénon, A. Information rate in humans during visuomotor tracking.
1717 *Entropy* **23**, 1–13 (2021).

1718 138. Uehara, S., Mawase, F., Therrien, A. S., Cherry-Allen, K. M. & Celnik, P.
1719 Interactions between motor exploration and reinforcement learning. *J.*
1720 *Neurophysiol.* **122**, 797–808 (2019).

1721 139. Rolls, E. T., Huang, C. C., Lin, C. P., Feng, J. & Joliot, M. Automated anatomical
1722 labelling atlas 3. *Neuroimage* **206**, 116189 (2020).

1723